Supplementary Information

Mice

Wild-type (WT) C57BL/6 and BALB/c mice were purchased from Walter and Eliza Hall Institute for Medical Research or bred in house. C57BL6 $Ptprc^a$ (CD45.1$^+$) mice, C57BL/6 CD39-deficient ($Cd39^{-/-}$) mice (1), C57BL/6 CD73-deficient ($Cd73^{-/-}$) mice, C57BL/6 Adenosine 2A receptor-deficient mice ($Adora2a^{-/-}$) (2); C57BL/6 Adenosine 2B receptor-deficient mice ($Adora2b^{-/-}$), C57BL/6 NALP3-deficient ($Nalp3^{-/-}$) mice, C57BL/6 P2X7-deficient ($P2X7^{-/-}$) mice (3), C57BL/6 ASC-deficient ($Pycard^{-/-}$) mice, C57BL/6 IL-18-deficient mice (Il18$^{-/-}$) (4), C57BL/6 IL-1 receptor-deficient mice ($Il1R^{-/-}$), C57BL/6 IFNγ-deficient mice (Ifng$^{-/-}$), C57BL/6 perforin-deficient ($Pfp^{-/-}$), C57BL/6 gld mutant (gld) and Nod-rag1-gamma c (NRG) mice were bred in-house and maintained at the QIMR Berghofer Medical Research Institute. Pmel-1 TCR Tg mice have been previously described (5). Mice greater than 6 weeks of age were sex-matched to the appropriate models. The number of mice in each group treatment or strain of mice for each experiment is indicated in the figure legends. In all studies, no mice were excluded based on pre-established criteria and randomization was only applied immediately pre-treatment in therapy experiments to ensure similar mean tumor size was the starting point. Experiments were conducted as approved by the QIMR Berghofer Medical Research Institute Animal Ethics Committee.

Cell Culture

Mouse CT26 colon adenocarcinoma and TUBO mammary carcinoma were cultured in RPMI 1640, supplemented with 10% Fetal Calf Serum (Bovogen), 1% Glutamine

(Gibco), and 1% Penicillin-Streptomycin (Gibco)(complete RPMI). The human SK-MEL-28 melanoma was routinely maintained in complete RPMI.

In vivo treatments

For mouse tumor models, clodronate-containing liposomes for the depletion of phagocytic cells and empty-control liposome preparations was used as described [clodrolip; sodium clodronate tetrahydrate, Farchemia SRL, Treviglio, Italy (6)]. Clodrolip and control liposomes were diluted in PBS and injected i.p. at 2 mg per 20 g body weight, 2 d prior to therapy. Subsequent doses of depleting and control liposome preparations (1 mg/20 g body weight) were administered every 2 d. Some groups of mice were neutralized for TRAIL (N2B2), CD11b (5C6), or IFNγ (H22) using the scheduling and dosing as indicated. Some mice were treated with cIg (I-536, Leinco), anti-mouse CD39 (B66, mIgG1, Tizona), anti-mouse CD39 (B66, mIgG1 D265A, Tizona), anti-mouse CD39 (Tz-617, mouse IgG1, Tizona), anti-mouse CD39 (Tz-619, mouse IgG1, Tizona), anti-CD73 (2C5; mIgG1, Tizona), anti-PD1 (RMP1-14), A2AR inhibitor (SCH58261)(Sigma-Aldrich), A2BR inhibitor (PSB1115)(Sigma Aldrich), and CD39 inhibitors (POM1 and ARL-67156)(Santa Cruz Biotechnology and Sigma Aldrich, respectively) with schedules and doses as indicated in the figure legends. For human tumor models, some groups of mice treated either: cIg (Palivizumab hG4, MedImmune), anti-CD39 (TTX-030; Tizona), anti-PD1 (Pembrolizumab, Merck) with schedules and doses as indicated in the figure legends.

Enzyme Histochemistry

Enzyme histochemistry (EHC) was performed on mouse MC38 tumors harvested on day 14 in OCT. Slides containing 5 μM OCT-embedded fresh frozen tissue were brought to RT before fixing in 4% PFA, then transferred to a chamber containing Trizma-maleate sucrose buffer (TMSB 9.5 g/L Trizma maleate, 80 g/L sucrose, pH 7.4) for 60 minutes. The slides were then incubated in substrate buffer containing TMSB with 0.5 mM $CaCl_2$, 0.25 mg/mL lead nitrate and ATP before washing with dH20. The lead orthophosphate precipitated in the course of nucleotidase activity was visualized as a brown deposit by incubating sections in 0.4% $(NH_4)_2S$ followed by three washes in TMSB. Slides were mounted with mounting medium (DAKO) and images were acquired using a digital Aperio slide scanner. Using Aperio ImageScope software, the representative images were captured and the mean of total pixel intensities across sample per unit area of the tumor tissues were calculated for each sample.

IL-18 ELISA

WT mice and $Nalp3^{-/-}$ mice were subcutaneously challenged with MC38 tumor cells (1 x 10^6). Mice were treated i.p. with anti-CD39 or cIg (200 µg) on day 8 after tumor inoculation. Tumor samples were collected 24 h post-treatment, followed by snap-freezing in liquid nitrogen. Frozen tumor samples were mechanically digested in the presence of T-PER Tissue Protein Extraction Reagent (Thermo Fisher Scientific) supplemented with Complete™ Protease Inhibitor Cocktail (Sigma Aldrich). IL-18 levels in tumor lysates were measured by sandwich ELISA using anti-mouse IL-18 mAb (clone 74, MBL international), and biotinylated anti-IL-18 (Clone 93-10C, MBL international), as capture and detection antibodies, respectively (7). Colorimetric

quantification was performed by HRP-streptavidin (Sigma Aldrich) and TMB substrate solution (eBioscience).

Flow cytometry

Tumors, tumor draining lymph nodes, and spleens were harvested from mice untreated or treated with control or therapeutic antibodies as indicated in the figure legends. Tumors and lymph nodes were minced and digested with 1 mg/mL collagenase IV (Worthington Biochemical) and 0.02 mg/mL DNase I (Roche) and homogenized to prepare single cell suspensions. Single cell suspensions of spleens were depleted of erythrocytes. For surface staining, cells were stained in phosphate buffered saline (PBS) containing 2% (v/v) FBS with anti-CD45.2 (104; BD biosciences) or anti-CD45.2 (30-F11; Thermofisher), anti-CD4 (RM4-5; Biolegend) or anti-CD4 (GK1.5; eBioscience), anti-CD8a (53-6.7; Biolegend), anti-TCRβ (H57-597; Biolegend), anti-NK1.1 (PK136; BD biosciences), anti-CD39 (Duha59; BioLegend), anti-CD73 (TY/23; BD Bioscience), OVA-tetramer (assembled with biotinylated KbOVA monomer from Prof Andrew Brooks Lab, the University of Melbourne and streptavidin from BD biosciences), anti-CD279 (29F.1A12; BioLegend), anti-Ly6G (1A8; BioLegend), anti-CD11b (M1/70; BioLegend), anti-CD11c (N418; eBioscience), anti-CD64 (X54-5/7.1; BioLegend), anti-MHC II (M5/114.15.2; eBioscience), anti-CD274 (10F.9G2; BioLegend), anti-P2X7R (1F11; BioLegend). For intracellular staining, surface-stained cells were fixed and permeabilized using the Foxp3/Transcription Factor Staining Buffer Set (eBioscience) or BD Cytofix/Cytoperm (BD Biosciences) according to the manufacturer's protocol and stained with anti-Foxp3 (FJK-16s, eBioscience), anti-IFNγ (XMG1.2; BioLegend), anti-Ki67 (16A8; BioLegend) or anti-Ki67 (B56; BD biosciences), and respective

isotype antibodies. For intracellular staining of IFNγ, cells were stimulated ex vivo with eBioscience™ Cell Stimulation Cocktail (plus protein transport inhibitors) for 4 h before surface staining. Populations defined in $CD45^+$ live cells: $CD8^+$ T cells, $TCRβ^+CD8^+$; $CD4^+Foxp3^-$ T cells, $TCRβ^+CD4^+Foxp3^-$; regulatory T cells (Treg), $TCRβ^+CD4^+Foxp3^+$; natural killer (NK) cells, $NK1.1^+TCRβ^-$; neutrophils, $Ly6G^+$; eosinophils, $Ly6G^-CD64^-MHCII^-CD11b^+SSC^{hi}$; macrophages, $Ly6G^-CD64^+MHCII^+$; dendritic cells (DC), $Ly6G^-CD64^-MHCII^+CD11c^+$; monocytes, $Ly6G^-CD64^{-/lo}MHCII^{-/lo}CD11b^{hi}SSC^{lo}$. Cells were acquired on the BD LSR Fortessa V (BD Biosciences) and analysis was carried out using FlowJo (Tree Star). Dead cells stained by 7-AAD (BioLegend) or Zombie Aqua (BioLegend) were excluded from analysis. Lymphoid and myeloid components were gated by markers indicated in Figure S7.

Adoptive transfer of gp100-specific mouse T cells

Cohorts of C57BL/6 WT or $Cd39^{-/-}$ mice were s.c. injected with HC.PmelKO.TYRP1-SFhg100 melanoma cells. The melanoma cell line HCmel12 was established from a primary melanoma in the $Hgf-CDK4^{R24C}$ mouse model by serial transplantation in our laboratory as previously described (8). The Pmel gene was knocked out using CRISPR/Cas9 technology to generate the HC.PmelKO melanoma monoclonal cell line. Using CRISPitope we generate HC.PmelKO cells expressing mScarlet fluorescent protein (S), a FLAG-Tag (F) and the human gp100 epitope [KVPRNQDWL ($hgp100_{25-33}$)] fused to TYRP1 to generate HC.PmelKO.TYRP1-SFhgp100 cells as described previously (Effern et al. submitted). Once melanomas were palpable, mice received a single dose of cyclophosphamide (2 mg i.p., Baxter) followed the next day by the adoptive transfer of 1×10^6 purified gp100-specific Pmel-1 T cells isolated from

the spleen of Pmel-1 TCRTg mice. On days 3,6 and 9 after cyclophosphamide all mice received intratumor injections of polyI:C/CpG (50 μg/mouse of each, Invivogen) as described previously (9). Mice were randomly allocated for antibody treatment on the day of cyclophosphamide injection. Therapeutic antibody treatment commenced as indicated and mIgG1 or anti-CD39 (B66) (200 µg each i.p.) was given every 3 or 4 days up to a maximum of 5 doses.

Statistical analysis

Statistical analysis was determined with Graphpad Prism 7 (GraphPad Software). A 1-tailed Mann-Whitney U test was used for comparisons of 2 groups. Significance of differences was also calculated by log-rank t test or Gehan-Breslow-Wilcoxon for Kaplan-Meier survival analysis or 2-way ANOVA as necessary. Tukey's multiple comparisons tests were utilized unless otherwise indicated. A Fisher's exact test was also used to determine significance of proportion of tumor free mice. Differences between groups are shown as the mean ± SEM. P values of less than 0.05 were considered statistically significant.

References

1.   Enjyoji K, Sevigny J, Lin Y, Frenette PS, Christie PD, Esch JS, 2nd, *et al.* Targeted disruption of cd39/ATP diphosphohydrolase results in disordered hemostasis and thromboregulation. Nat Med **1999**;5(9):1010-7 doi 10.1038/12447.
2.   Young A, Ngiow SF, Barkauskas DS, Sult E, Hay C, Blake SJ, *et al.* Co-inhibition of CD73 and A2AR adenosine signaling improves anti-tumor immune responses. Cancer Cell **2016**;30(3):391-403 doi 10.1016/j.ccell.2016.06.025.
3.   Solle M, Labasi J, Perregaux DG, Stam E, Petrushova N, Koller BH, *et al.* Altered cytokine production in mice lacking P2X(7) receptors. J Biol Chem **2001**;276(1):125-32 doi 10.1074/jbc.M006781200.
4.   Takeda K, Tsutsui H, Yoshimoto T, Adachi O, Yoshida N, Kishimoto T, *et al.* Defective NK cell activity and Th1 response in IL-18-deficient mice. Immunity **1998**;8(3):383-90.
5.   Landsberg J, Kohlmeyer J, Renn M, Bald T, Rogava M, Cron M, *et al.* Melanomas resist T-cell therapy through inflammation-induced reversible dedifferentiation. Nature **2012**;490(7420):412-6 doi 10.1038/nature11538.
6.   Haynes NM, Hawkins ED, Li M, McLaughlin NM, Hammerling GJ, Schwendener R, *et al.* CD11c+ dendritic cells and B cells contribute to the tumoricidal activity of anti-DR5 antibody therapy in established tumors. J Immunol **2010**;185(1):532-41 doi 10.4049/jimmunol.0903624.
7.   Nakamura K, Kassem S, Cleynen A, Chretien ML, Guillerey C, Putz EM, *et al.* Dysregulated IL-18 is a key driver of immunosuppression and a possible therapeutic target in the multiple myeloma microenvironment. Cancer Cell **2018**;33(4):634-48 e5 doi 10.1016/j.ccell.2018.02.007.
8.   Bald T, Quast T, Landsberg J, Rogava M, Glodde N, Lopez-Ramos D, *et al.* Ultraviolet-radiation-induced inflammation promotes angiotropism and metastasis in melanoma. Nature **2014**;507(7490):109-13 doi 10.1038/nature13111.
9.   Glodde N, Bald T, van den Boorn-Konijnenberg D, Nakamura K, O'Donnell JS, Szczepanski S, *et al.* Reactive neutrophil responses dependent on the receptor tyrosine kinase c-MET limit cancer immunotherapy. Immunity **2017**;47(4):789-802 e9 doi 10.1016/j.immuni.2017.09.012.

Figure S1

A
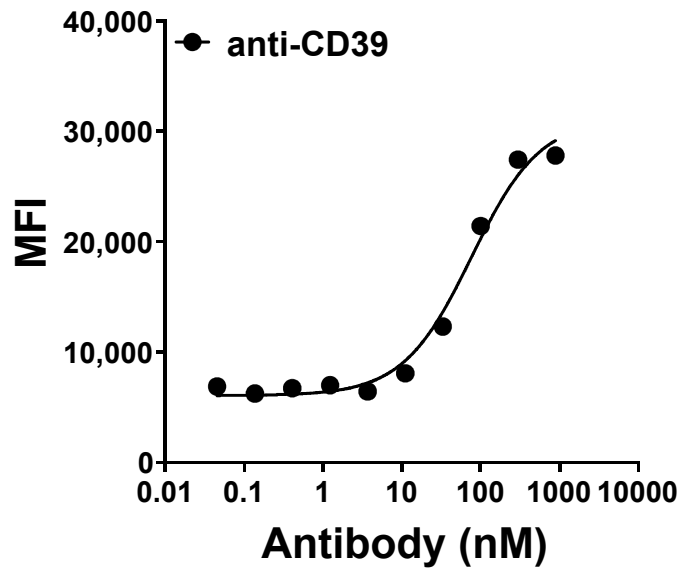
B
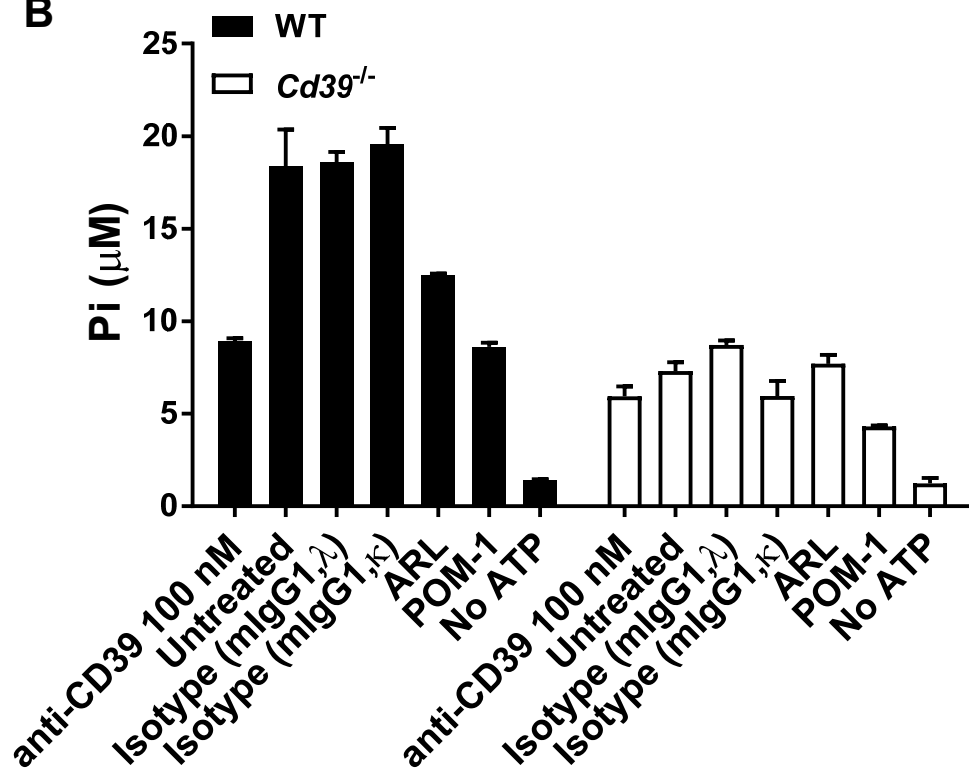
Supplementary Figure Legends

Figure S1. Anti-CD39 mAb binds to BCL1 cells with high affinity and blocks CD39 enzymatic activity in splenocytes from CD39$^{-/-}$ mice. The graphs shown represent the binding affinity of anti-CD39 antibody (B66) to BCL1 cells by titration **(A)** and blockade of CD39 enzymatic activity by isotype antibody controls, B66, ARL and POM-1 in the presence of ATP or absence (no ATP) in splenocytes from WT (closed squares) and CD39$^{-/-}$ (open squares) mice measured by phosphate release **(B)**. In addition, anti-CD39 was determined by Biolayer Interferometry to bind to recombinant mCD39-ECD with a monovalent K_D of 2.65 nM.

Figure S2

A

clg
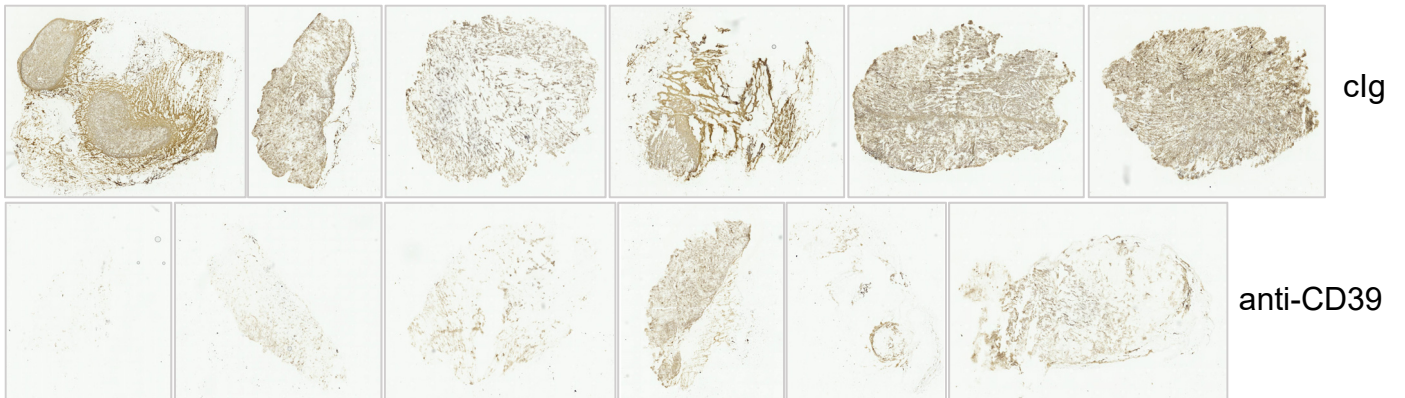
anti-CD39

B
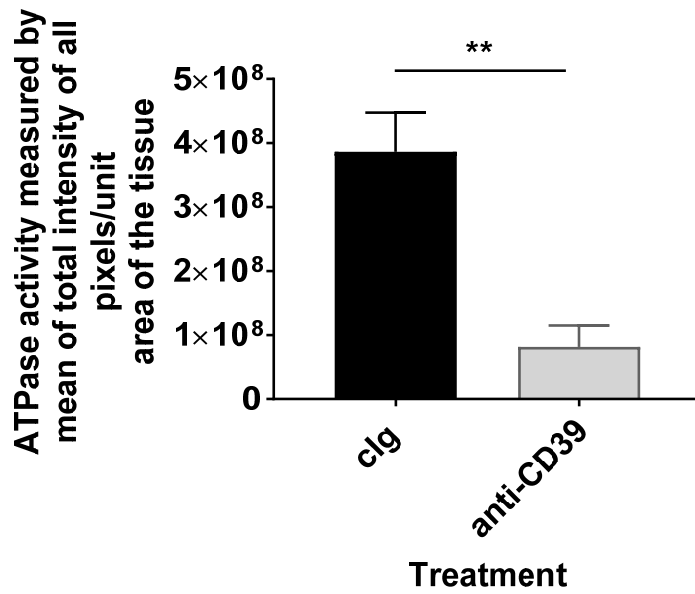
C
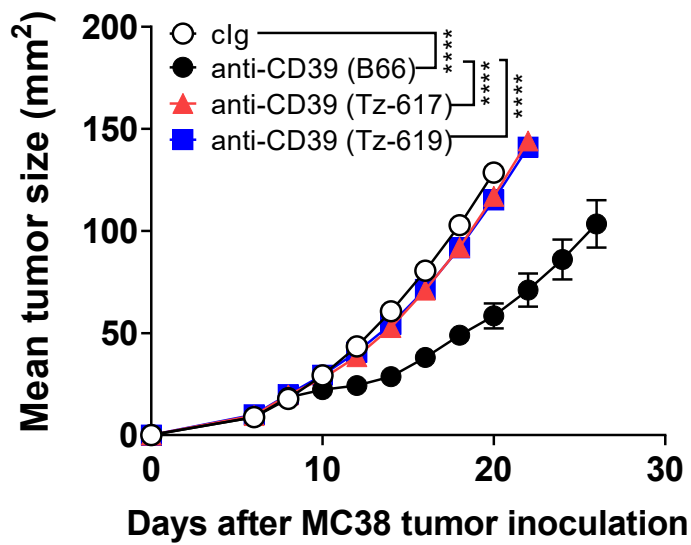
Figure S2. Groups (n = 6/group) of WT mice were injected s.c. with MC38 colon adenocarcinoma cells (1 x 10^5) on day 0 and treated i.p. with clg (200 μg) or anti-CD39 (200 μg) on day 12. The tumor samples were harvested 48 h post-treatment in OCT and EHC was performed as described in Methods. **(A)** Representative EHC images and **(B)** the quantification of staining intensity represented as the means of total pixel intensities across samples per unit area of the tumor tissues, showing reduced ATPase activity in the anti-CD39-treated group compared to clg-treated group. Significant differences were determined by Mann-Whitney test (** $P < 0.01$). Representative of two experiments performed **(C)** Groups (n = 10/group) of WT mice were injected s.c. with MC38 (1 x 10^5) colon adenocarcinoma cells on day 0 and treated i.p with clg (200 μg) or various anti-CD39 (B66, Tz-617, Tz-619, 200 μg) on days 8, 11, 14, and 17. Representative of two experiments performed. Tumor sizes (mm^2) were measured at the indicated time points and presented as mean ± SEM. All experiments were performed once unless indicated. Significant differences among treatment groups were determined by a two-way ANOVA, followed by Tukey's multiple comparison test (**** $p < 0.0001$).

Figure S3

A
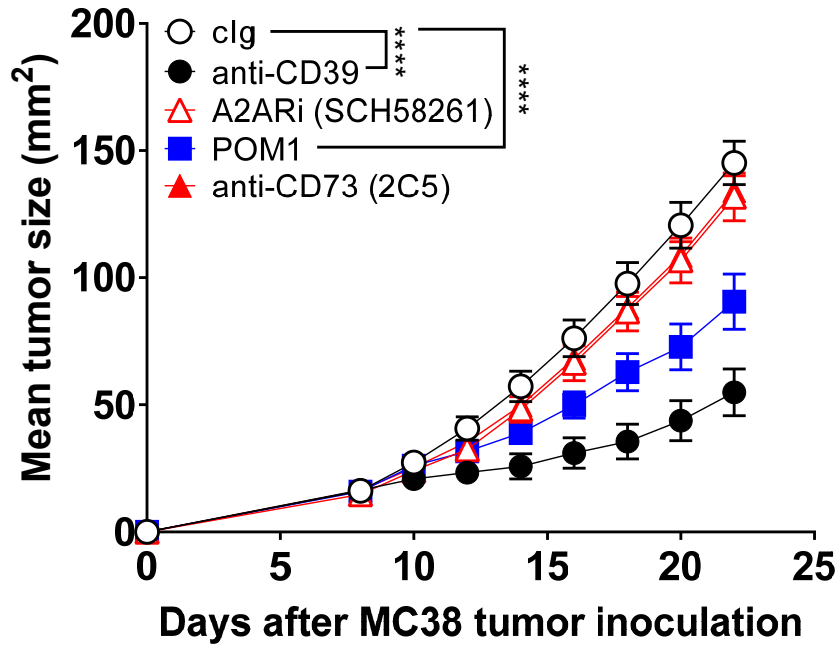
B
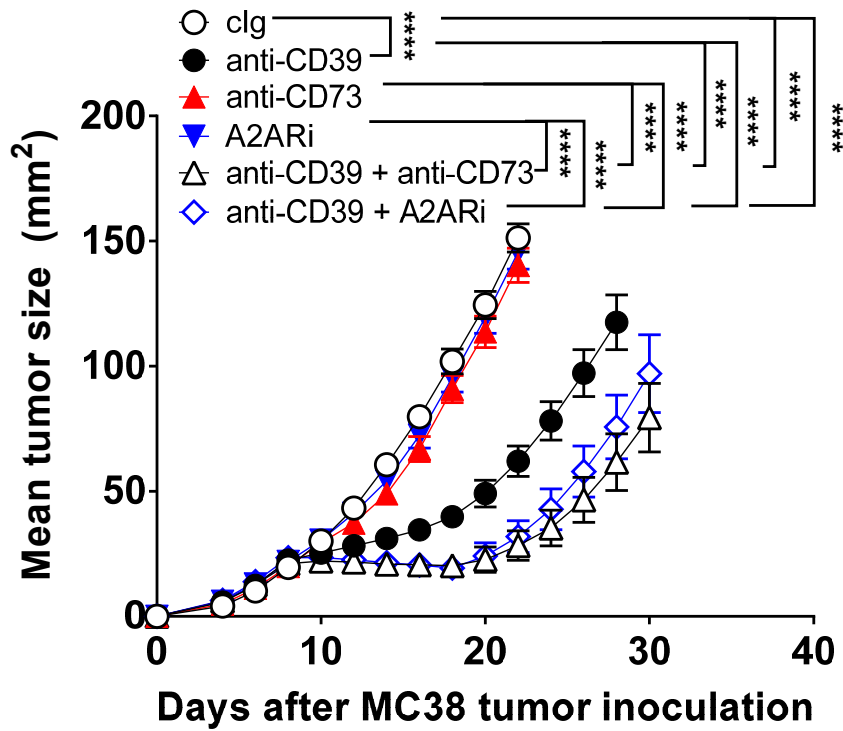
Figure S3. Anti-CD39 mAb is more effective than POM-1 in suppressing MC38 tumor growth. (A) Groups (n = 5/group) of C57BL/6 WT mice were injected s.c. with MC38 (1 x 10^5) colon adenocarcinoma cells and treated i.p. with cIg (200 μg) anti-CD39 (200 μg), A2ARi (SCH58261, 10 mg/kg) on days 8, 11, 14 and 17, or 250 μg POM-1 on days 8, 10, 12, 14, 16 and 18. **(B)** Adenosine blockade further improves anti-CD39 control of MC38 tumor growth. Groups (n = 10/group) of WT mice were injected s.c. with MC38 (1 x 10^5) colon adenocarcinoma cells on day 0 and treated i.p with cIg (200 μg), anti-CD39 (200 μg), anti-CD73 (200 μg), A2ARi (SCH58261)(10 mg/kg) or combination of these as indicated on days 8, 11, 14, and 17. This experiment is representative of two performed. Tumor sizes (mm^2) were measured at the indicated time points and presented as mean ± SEM. Significant differences among treatment groups were determined by a two-way ANOVA, followed by Tukey's multiple comparison test (**** $P < 0.0001$).

Figure S4
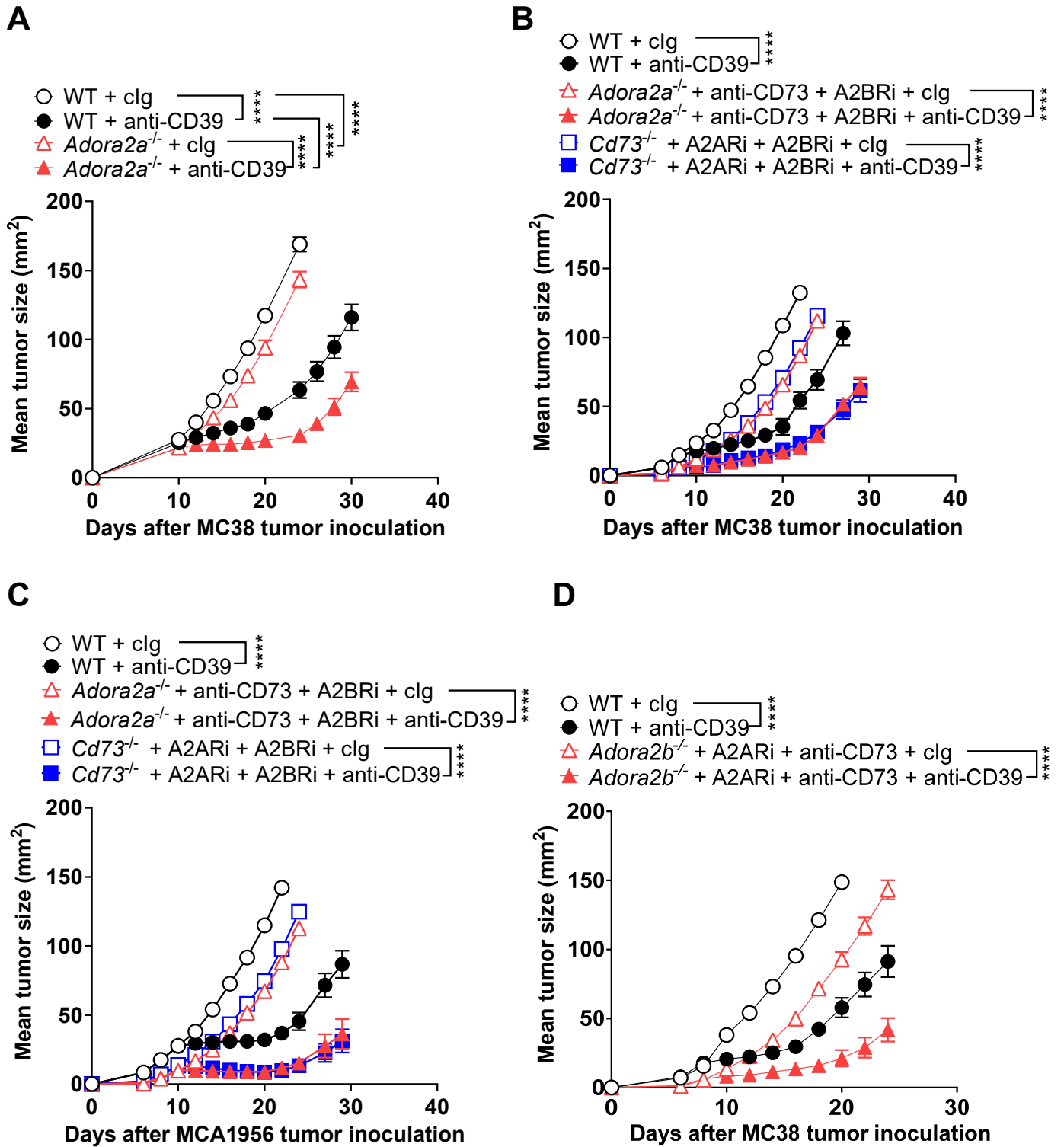
Figure S4. Combination of anti-CD39 with adenosine blockade. (A) Groups (n = 9-10/group) of C57BL/6 WT or *Adora2a*^{-/-} mice were injected subcutaneously (s.c.) with MC38 (1 x 10^5) colon adenocarcinoma cells and treated i.p. with cIg (200 μg) anti-CD39 (200 μg) on days 10, 13, 16 and 19. **(B)** Groups (n = 10/group) of WT, *Adora2a*^{-/-}, and *Cd73*^{-/-} mice were injected s.c. with MC38 (1 x 10^5) colon adenocarcinoma cells on day 0. *Adora2a*^{-/-} mice were treated i.p with a combination of anti-CD73 (200 μg) and (A2BR inhibitor) PSB1115 (1 mg/kg) and *Cd73*^{-/-} mice treated with a combination of A2AR inhibitor (SCH58261) (10 mg/kg) and (A2BR inhibitor) (PSB1115) (1 mg/kg) on days 0, 3, 6, 9, 12, 15 and 18. All groups of mice were also treated i.p with cIg (200 μg) or anti-CD39 (200 μg) on days 8, 11, 14, and 17. **(C)** Groups (n = 7-8/group) of WT, *Adora2a*^{-/-}, and *Cd73*^{-/-} mice were injected s.c. with MCA1956 (1 x 10^6) colon adenocarcinoma cells on day 0. *Adora2a*^{-/-} mice were treated i.p with a combination of anti-CD73 (200 μg) and (A2BR inhibitor) (PSB1115) (1 mg/kg) and *Cd73*^{-/-} mice treated with a combination of A2AR inhibitor (SCH58261) (10 mg/kg) and PSB1115 (A2BR inhibitor) (1 mg/kg) on days 0, 3, 6, 9, 12, 15 and 18. All groups of mice were also treated i.p with cIg (200 μg) or anti-CD39 (200 μg) on days 10, 13, 16, and 19. **(D)** Groups (n = 5/group) of WT and *Adora2b*^{-/-} mice were injected s.c. with MC38 (1 x 10^5) colon adenocarcinoma cells on day 0. *Adora2b*^{-/-} mice were treated i.p with a combination of anti-CD73 (200 μg) and SCH58261 (10 mg/kg) on days 0, 3, 6, 9, 12, 15 and 18. All groups of mice were also treated i.p with cIg (200 μg) or anti-CD39 (200 μg) on days 8, 11, 14, and 17. Tumor sizes (mm^2) were measured at the indicated time points and presented as mean ± SEM. Significant differences among treatment groups were determined by a two-way ANOVA, followed by Tukey's multiple comparison test (**** $P < 0.0001$).

Figure S5

A
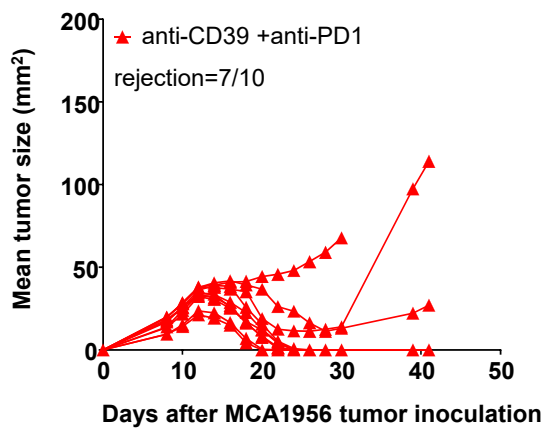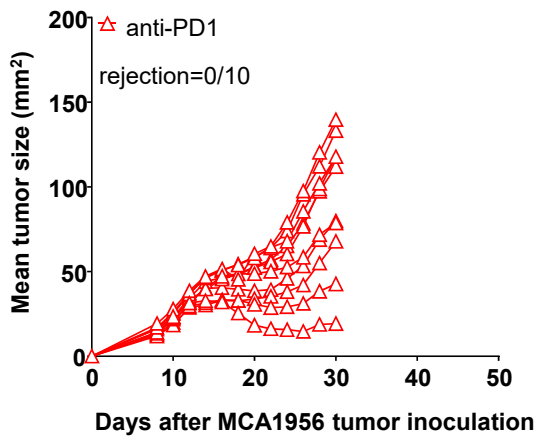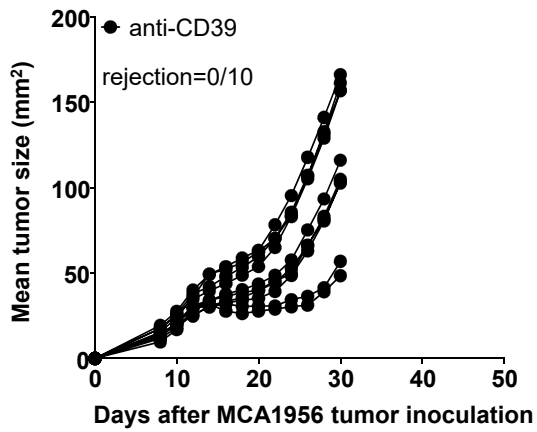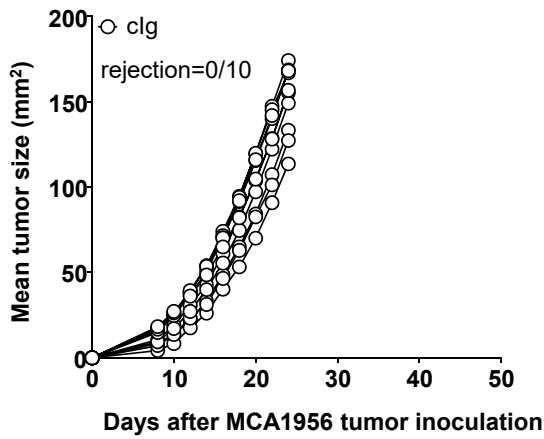
B
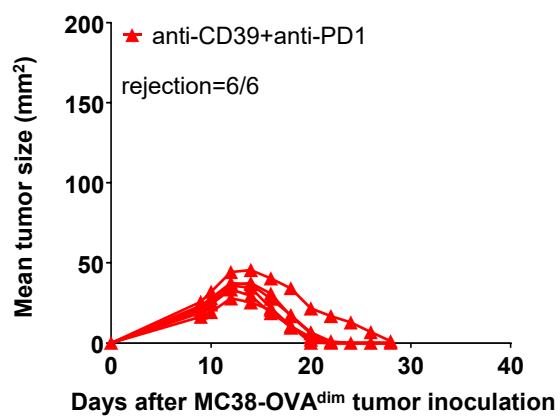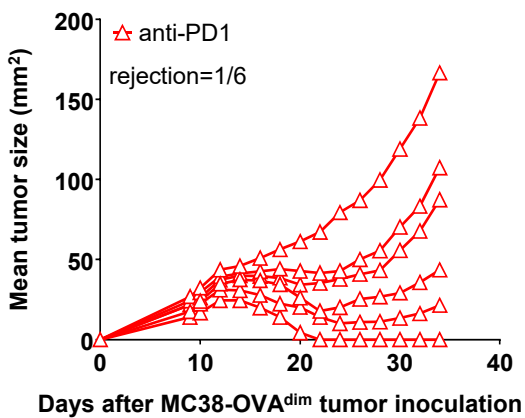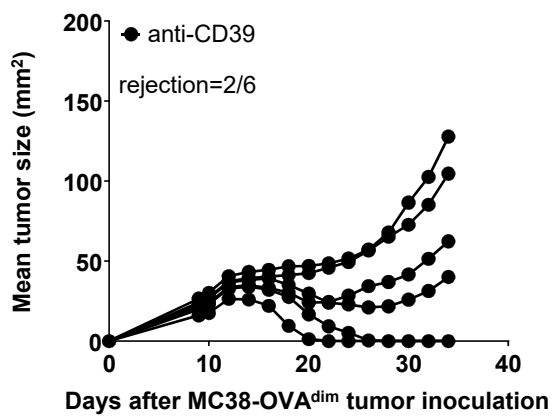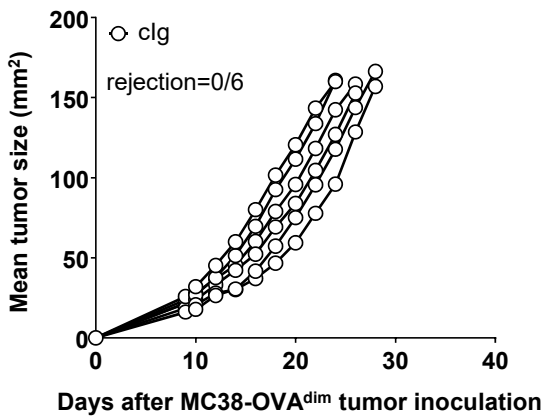
Figure S5. Individual tumor growth curves from anti-CD39- and anti-PD1-treated mice. Individual growth curves plotted from mice in **(A)** Figure 1G (MCA1956) and **(B)** Figure 1H (MC38-OVA^{dim}). Tumor rejection rates are as indicated for each panel/treatment group.

Figure S6

A

B

C
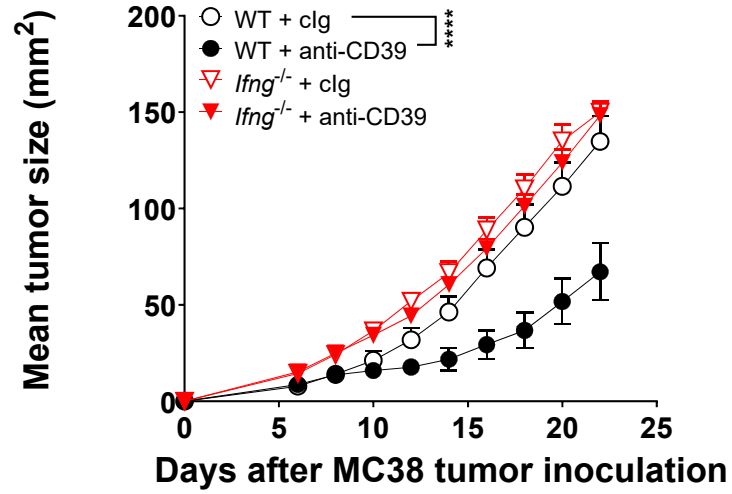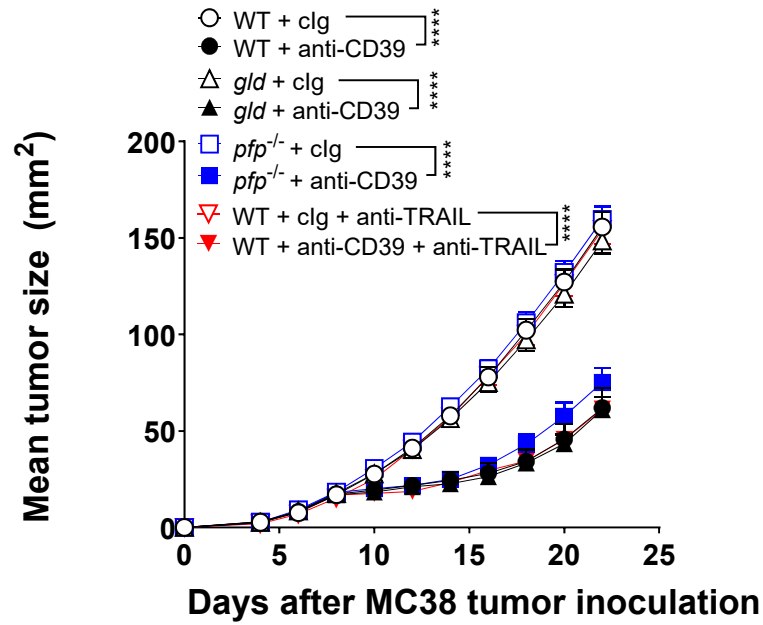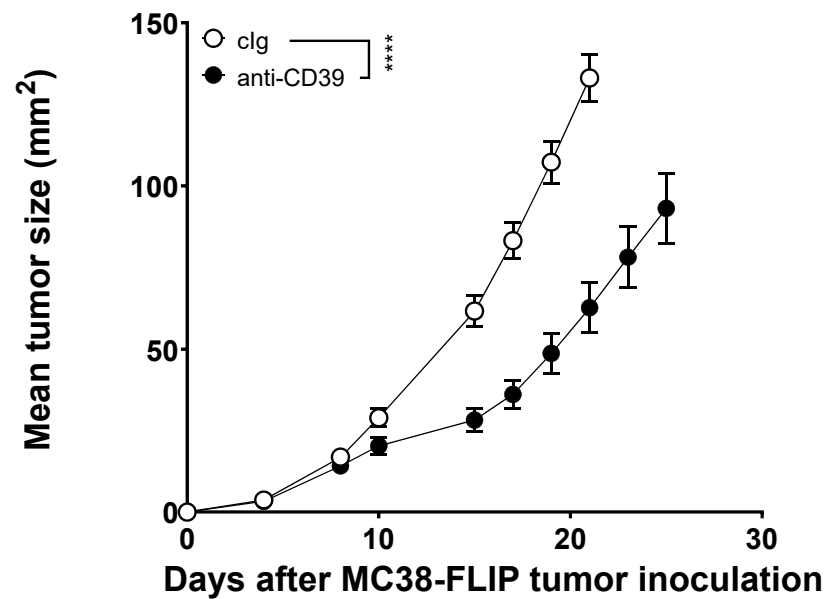
Figure S6. (A) IFN-γ-dependent MC38 tumor growth control by anti-CD39 mAb.
Groups (n= 8-10/group) of C57BL/6 WT or *Ifng*^{-/-} mice were injected s.c. with MC38
(1×10^5) colon adenocarcinoma cells and treated i.p. with cIg (200 μg) or anti-CD39
mAb (200 μg) on days 8, 11, 14 and 18. **(B-C) Lymphocyte cytotoxic mechanisms
were not required for the efficacy of anti-CD39 mAb. (B)** Groups (n = 5/group) of
WT, *pfp*^{-/-}, or *gld* mice were injected s.c. with MC38 (1×10^5) colon adenocarcinoma
cells on day 0 and treated i.p with cIg (200 μg) or anti-CD39 (200 μg) on days 8, 11,
14, and 17. WT mice additionally received i.p. either cIg (250 μg) or anti-TRAIL
(N2B2, 250 μg) on days 7, 8, 12, 14, 17, and 21. **(C)** Groups (n = 10/group) of WT
mice were injected s.c. with MC38-FLIP (1×10^5) colon adenocarcinoma cells on day
0 and treated i.p with cIg (200 μg) or anti-CD39 (200 μg) on days 8, 11, 15, and 17.
Tumor sizes (mm^2) were measured at the indicated time points and presented as
mean ± SEM. Experiments in A-C performed once. Significant differences among
treatment groups were determined by a two-way ANOVA, followed by Tukey's
multiple comparison test (**** P < 0.0001).

Figure S7

Lymphocyte Panel
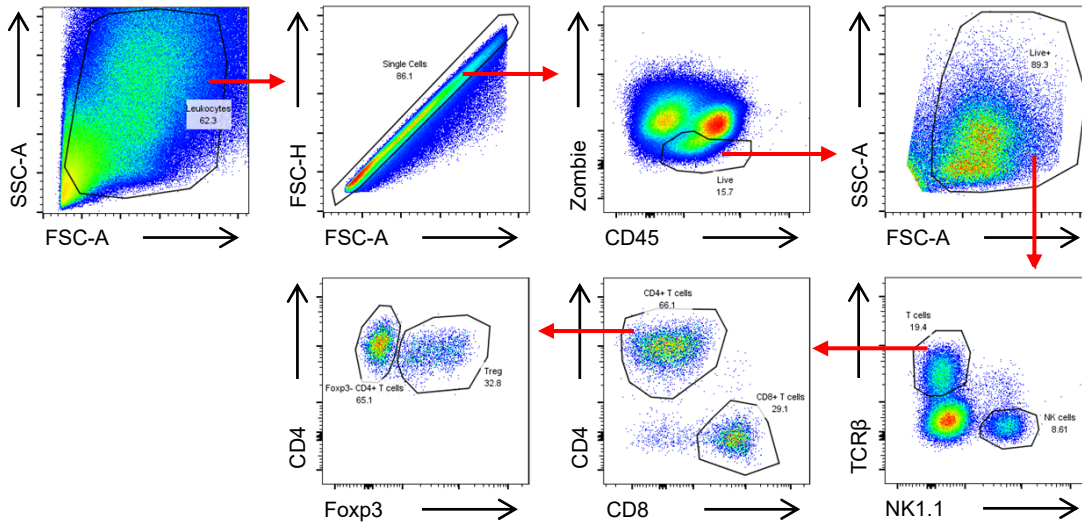
Myeloid Panel
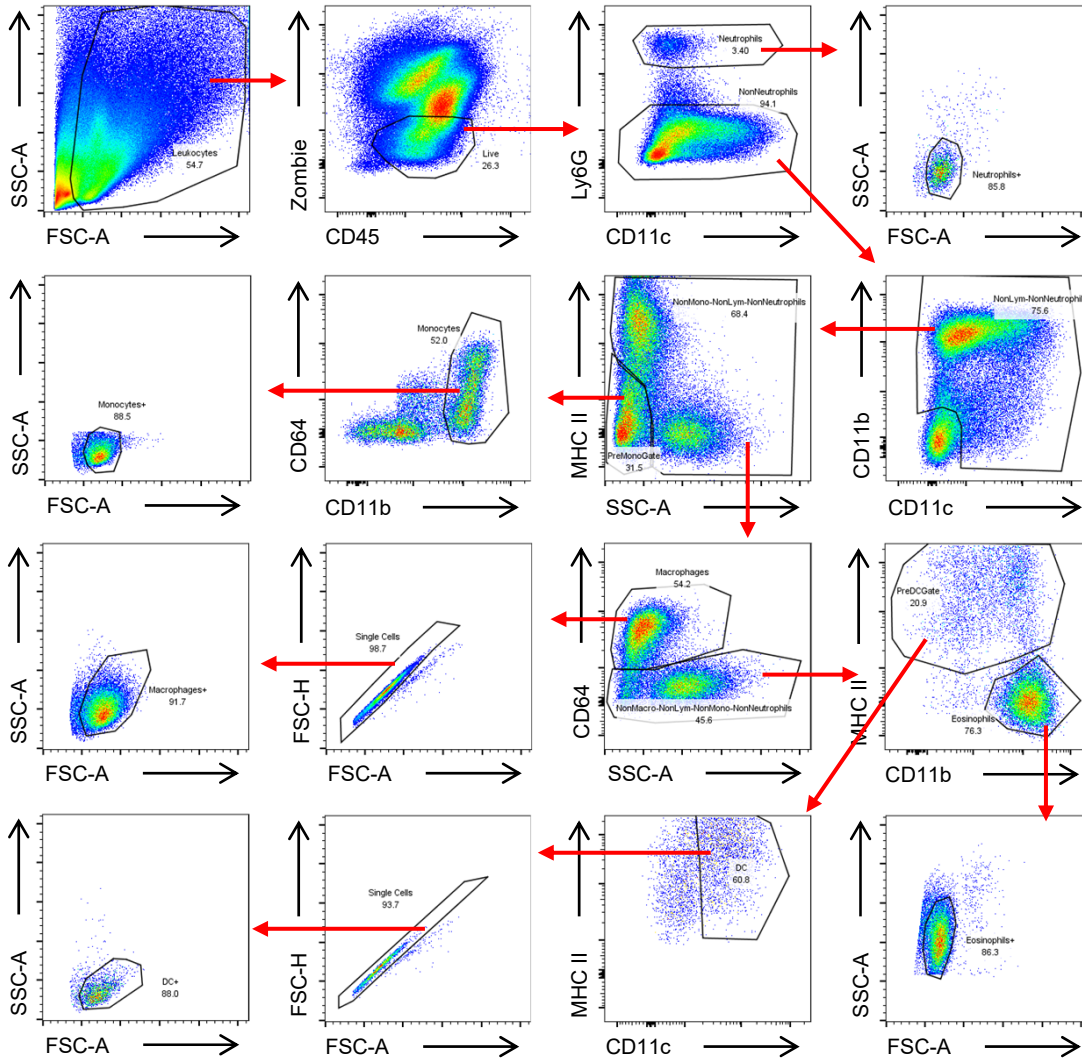
Figure S7. Gating strategies for different populations in FACS analyses. MC38 tumor samples are shown here as examples. For lymphocyte panel, CD45$^+$ live cells were gated out from single cells of general leukocyte size. Another gate in forward/side scatter was added to further exclude debris. After that, NK cells were gated out as NK1.1$^+$TCRb$^-$, CD8 T cells were gated as NK1.1$^-$TCRb$^+$CD8$^+$, Treg as NK1.1$^-$TCRb$^+$CD4$^+$Foxp3$^+$, and Foxp3$^-$ CD4 T cells as NK1.1$^-$TCRb$^+$CD4$^+$Foxp3$^-$. For myeloid panel, CD45$^+$ live cells were gated out from leukocytes. Neutrophils were defined as Ly6G$^+$. CD11b$^-$CD11c$^-$ lymphocytes were excluded from Ly6G$^-$ populations. From there, monocytes were defined as MHCII$^{-/low}$SSC^{low}CD11b^{high}CD64$^{low/+}$, macrophages were defined as MHCII$^+$CD64$^+$, eosinophils as MHCII$^-$CD64$^-$CD11b^{high}, dendritic cells as MHCII$^+$CD64$^-$CD11c$^+$. Additional gates in forward and side scatter were added for each of the populations to further exclude doublets and debris.

Figure S8
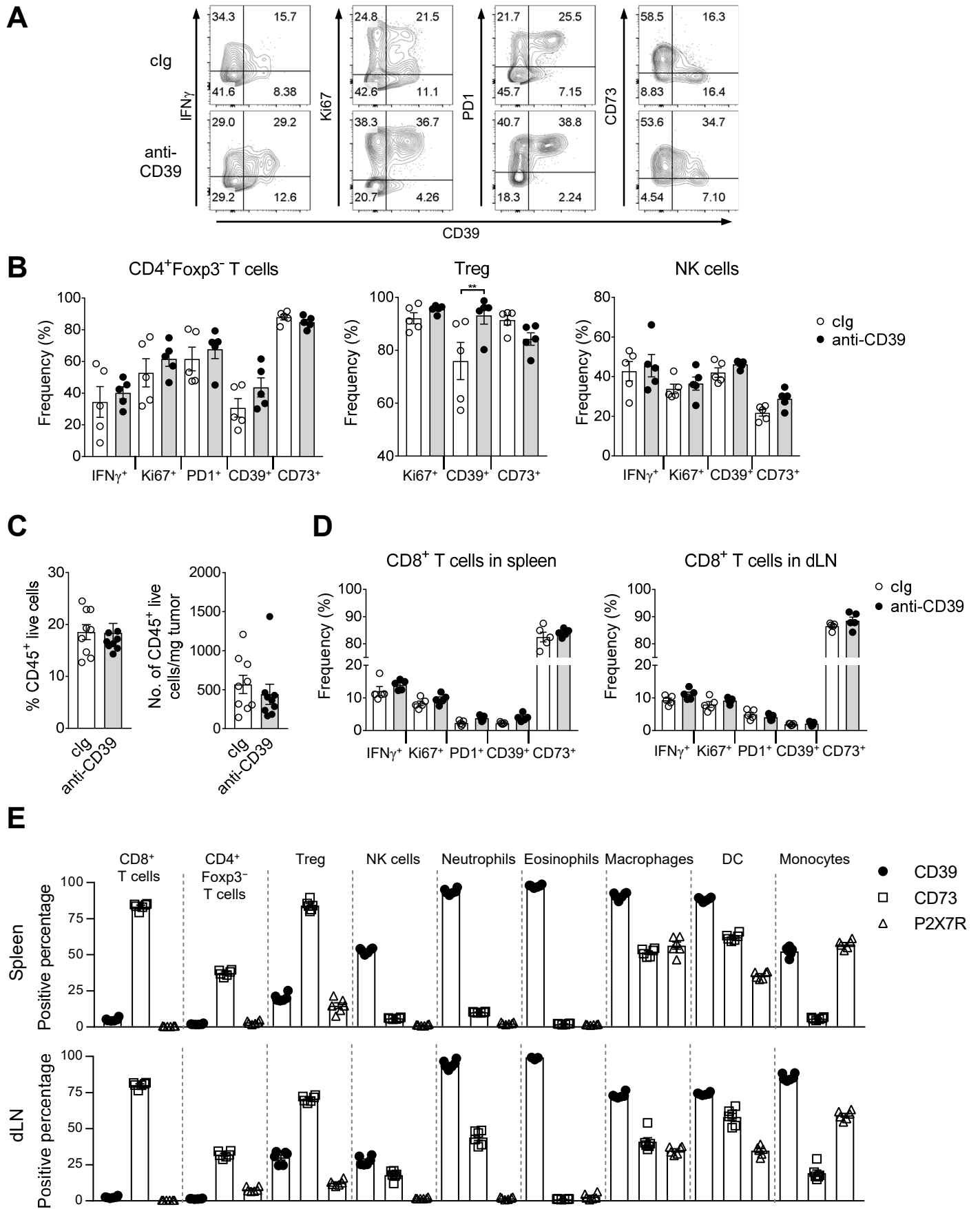
Figure S8. Anti-CD39 treatment modulates the phenotypic features and function of immune cells. From the same experiments as Fig. 2F, 2G and Fig. 4B, groups (n = 4–8/group) of WT mice were injected s.c. with (**A-E**) MC38 (1 x 10^5) colon adenocarcinoma cells on day 0. Mice were untreated (**E**) or treated i.p. with cIg (200 µg) or anti-CD39 (200 µg) on day 7 (**A–D**). Samples of tumor, spleen, and tumor draining lymph node (dLN) were collected on day 8 (**E**) or 48 h after mAb injection (**A-D**) and processed for single cell suspensions then subjected to flow cytometry with (**A-D**) or without (**E**) ex-vivo stimulation for 4 h. **A,** Representative FACS plots showing expression of CD39 and indicated surface and intracellular molecules on tumor-infiltrating CD8$^+$ T cells. **B,** Frequencies of MC38 tumor-infiltrating CD4$^+$Foxp3$^-$ T cells, Treg cells, and NK cells expressing the indicated surface and intracellular molecules and presented as mean ± SEM with individual values shown. **C,** Frequencies and numbers of MC38 tumor infiltrating leukocyte. **D,** Frequencies of CD8$^+$ T cells from the spleen or dLN of MC38-tumor bearing mice expressing the indicated surface and intracellular molecules and presented as the mean ± SEM with individual values shown. **E,** Summary bar graphs of frequencies of immune cell subsets expressing CD39, CD73 and P2X7R in the spleen and tumor draining lymph node of MC38-bearing mice, (mean ± SEM). Significant differences between the indicated groups were determined by a two-way ANOVA, followed by Sidak's multiple comparison test (**B** and **D**) or Mann-Whitney test (**C**). Data from (**C**) are pooled from two experiments while the remaining parts represent one experiment. (**B**) ** P < 0.01.

Figure S9

A

GSEA on Hallmark gene sets

Pathway (y-axis), Normalized Enrichment Score (NES) (x-axis)

Pathways (top to bottom):
HALLMARK_OXIDATIVE_PHOSPHORYLATION
HALLMARK_MYOGENESIS
HALLMARK_MYC_TARGETS_V1
HALLMARK_DNA_REPAIR
HALLMARK_INTERFERON_ALPHA_RESPONSE
HALLMARK_REACTIVE_OXIGEN_SPECIES_PATHWAY
HALLMARK_ALLOGRAFT_REJECTION
HALLMARK_G2M_CHECKPOINT
HALLMARK_HEME_METABOLISM
HALLMARK_HYPOXIA
HALLMARK_IL2_STAT5_SIGNALING
HALLMARK_EPITHELIAL_MESENCHYMAL_TRANSITION
HALLMARK_TNFA_SIGNALING_VIA_NFKB
HALLMARK_WNT_BETA_CATENIN_SIGNALING
HALLMARK_KRAS_SIGNALING_UP
HALLMARK_TGF_BETA_SIGNALING
HALLMARK_ESTROGEN_RESPONSE_EARLY
HALLMARK_MITOTIC_SPINDLE
HALLMARK_UV_RESPONSE_DN

FDR < 0.05
TRUE

B

Genes (top to bottom): Met, Il6ra, Tgfbr2, Ptgs2, Hgf, Vegfa, Nos2, Cd274, Adam17, Cybb, Csf1

Sample type: cIG, anti-CD39
Counts (log2): −1 −0.5 0 0.5 1

C

Genes (top to bottom): Ccr7, Ccl5, Nfkbid, Cd3e, Lat, Zap70, Socs1, Cd3d, Cd2, Lck, Lax1

Sample type: cIg, anti-CD39
Counts (log2): −1 −0.5 0 0.5 1

Figure S9. (A) Gene-set enrichment analysis of MC38 tumors treated with cIg compared to anti-CD39. From Fig. 3C, significantly regulated Hallmark gene sets between anti-CD39- and cIg-treated MC38 tumors (FDR < 0.05). **(B)** Heatmap of expression of key genes within immune suppression signature. **(C)** Heatmap of expression of key genes within T-cell activation signature.
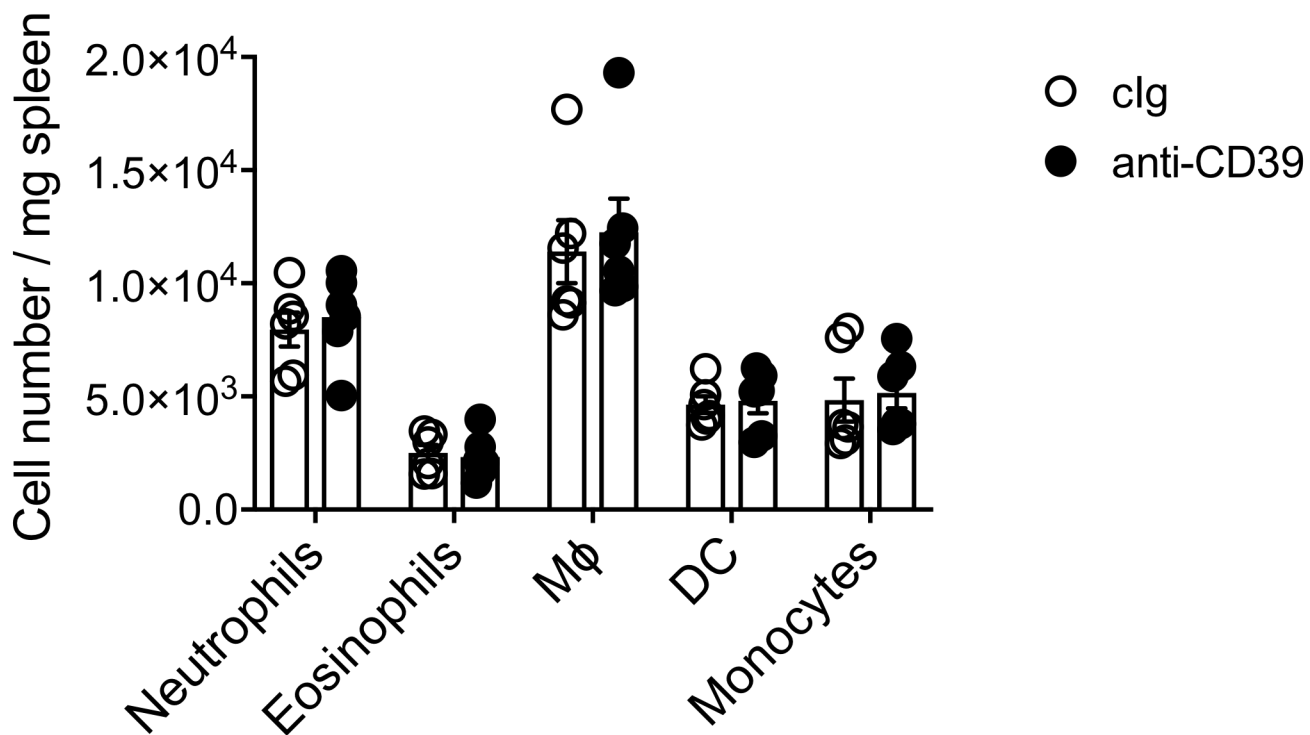
Figure S10. Flow cytometry shows no macrophage reduction in spleen after anti-CD39 treatment. From the same experiments as Figure 3D, groups (n = 6/group) of WT mice were injected s.c. with MC38 (1 x 10^5) colon adenocarcinoma cells on day 0 and treated i.p. with cIg (200 μg) or anti-CD39 (200 μg) on day 7. Spleen samples were collected on day 9 and processed for single cell suspensions then subjected to flow cytometry. Summary bar graphs of numbers of myeloid populations in spleen, as mean ± SEM with individual values shown. Data represents one experiment.

Figure S11

A

- ○ cIg + cIg
- ● cIg + anti-CD39
- △ cIg + clodronate
- ▲ anti-CD39 + clodronate
- □ cIg + control liposomes
- ■ anti-CD39 + control liposomes
- ▽ cIg + anti-CD11b
- ▼ anti-CD39 + anti-CD11b

****

**

****

ns

Mean tumor size (mm^2)

Days after MC38 tumor inoculation

B

- ○ cIg + cIg
- ● anti-CD39 + cIg
- △ cIg + anti-CD11b
- ▲ anti-CD39 + anti-CD11b
- ▽ cIg + anti-Ly-6G
- ▼ anti-CD39 + anti-Ly-6G

****

ns

****

Mean tumor size (mm^2)

Days after MC38 tumor inoculation

Figure S11. Anti-CD39 mAb efficacy requires CD11b and myeloid cells. **(A)** Groups (n = 5/group) of WT mice were injected s.c. with MC38 (1 x 10^5) colon adenocarcinoma cells on day 0 and treated i.p with anti-CD39 (200 μg) or cIg (200 μg) on days 8, 11, 14, and 17. Some groups of mice additionally received cIg or anti-CD11b (5C6) (300 μg i.p.) on days 7,8,15, and 21, or clodronate or control liposomes on days 6 (2 mg/20 g mouse), 8 (1 mg/20 g mouse thereafter), 10, 12, and 14. **(B)** Groups (n = 6/group) of WT mice were injected s.c. with MC38 (1 x 10^5) colon adenocarcinoma cells on day 0 and treated i.p with anti-CD39 (200 μg) or cIg (200 μg) on days 8, 11, 14, and 17. Some groups of mice additionally received cIg, anti-CD11b (5C6) or anti-Ly-6G (1A8) (300 μg i.p.) on days 7, 8, 15, and 24. Tumor sizes (mm^2) were measured at the indicated time points and presented as mean ± SEM. Experiment was performed once. Significant differences among treatment groups were determined by a two-way ANOVA, followed by Tukey's multiple comparison test (** $P < 0.01$; **** $P < 0.0001$).

Figure S12

A

B
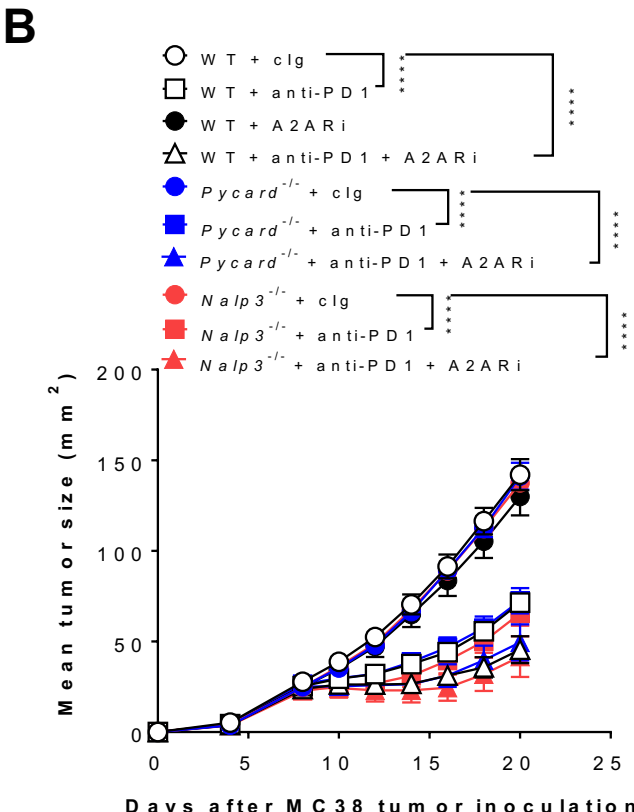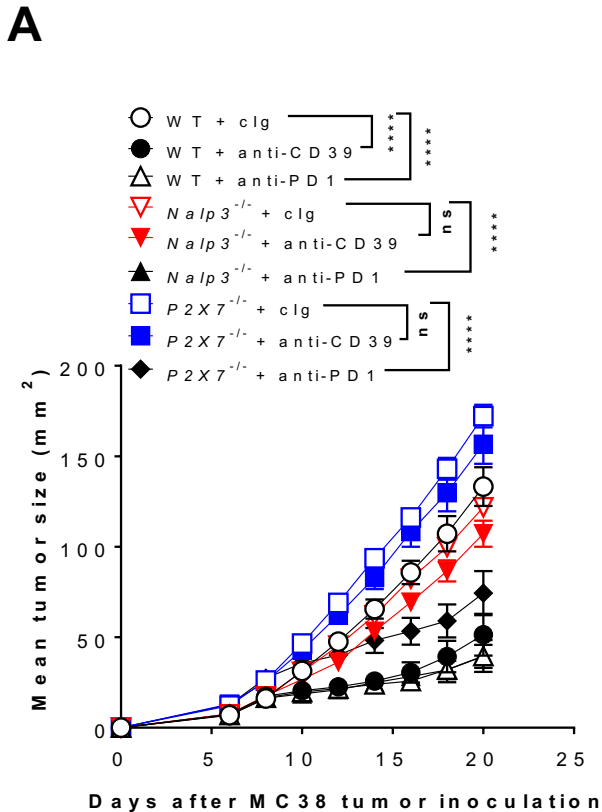
Figure S12. Anti-PD1 and SCH58261 efficacy is NALP3-independent. (A) Groups (n = 4-6/group) of WT, *P2X7*^{-/-}, and *Nalp3*^{-/-} mice were injected s.c. with MC38 (1 x 10^5) colon adenocarcinoma cells on day 0 and treated i.p with cIg (200 μg), anti-CD39 (200 μg), or anti-PD1 (250 μg) on days 8, 11, 14, and 17. **(B)** Groups (n = 5-6/group) of WT, *Pycard*^{-/-}, and *Nalp3*^{-/-} mice were injected s.c. with MC38 (1 x 10^5) colon adenocarcinoma cells on day 0 and treated i.p with cIg (200 μg), anti-PD1 (250 μg) or anti-PD1 (250 μg) and A2AR inhibitor (SCH58261) (10 mg/kg) on days 8, 11, 14, and 17. Tumor sizes (mm^2) were measured at the indicated time points and presented as mean ± SEM. Experiments performed once. Significant differences among treatment groups were determined by a two-way ANOVA, followed by Tukey's multiple comparison test (**** P < 0.0001, ns = not significant).

Figure S13

A
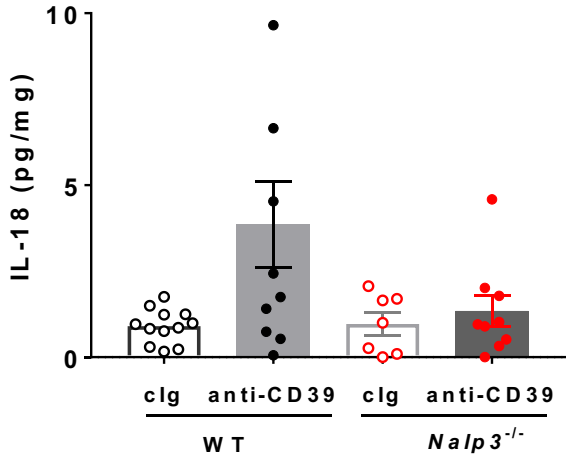
B
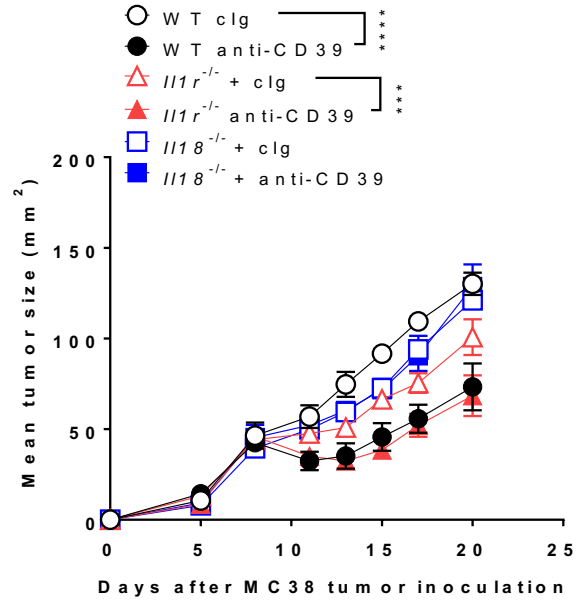
C
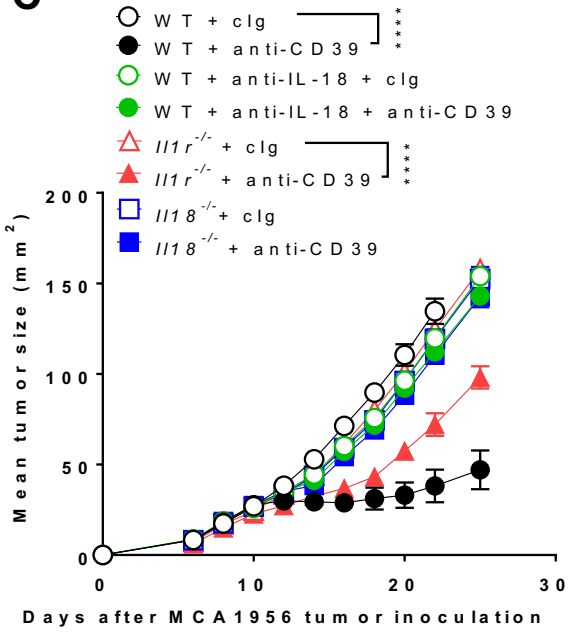
Figure S13. Role of IL-18 in mechanism of action of anti-CD39. (A) Inflammasome IL-18 production in MC38 tumors after anti-CD39 mAb. Groups (n = 7-9/group) of WT and *Nalp3*$^{-/-}$ mice were injected s.c. with MC38 (1 x 10^5) colon adenocarcinoma cells on day 0 and treated i.p with cIg (200 μg) or anti-CD39 (200 μg) on day 8. Tumor lysates were prepared 24 h after antibody treatment and IL-18 levels were determined by ELISA. This experiment is pooled from two performed. **(B)** Groups (n = 4/group) of WT, *Il1r*$^{-/-}$, or *Il18*$^{-/-}$ mice were injected s.c. with MC38 (5 x 10^5) colon adenocarcinoma cells on day 0 and treated i.p with cIg (200 μg) or anti-CD39 (200 μg) on days 8, 11, and 14. **(C)** Groups (n = 5/group) of WT, *Il1r*$^{-/-}$, or *Il18*$^{-/-}$ mice were injected s.c. with MCA1956 (1 x 10^6) sarcoma cells on day 0 and treated i.p with cIg (200 μg) or anti-CD39 (200 μg) on days 10, 13, 16, and 19. WT mice additionally received i.p either cIg (250 μg) or anti-IL-18 (250 μg) on days 9, 10, 17, and 24 after tumor inoculation. **(B-C)** Experiments performed twice each. Significant differences among treatment groups were determined by a two-way ANOVA, followed by Tukey's multiple comparison test (* P < 0.05, *** P < 0.001, **** P < 0.0001).

Figure S14
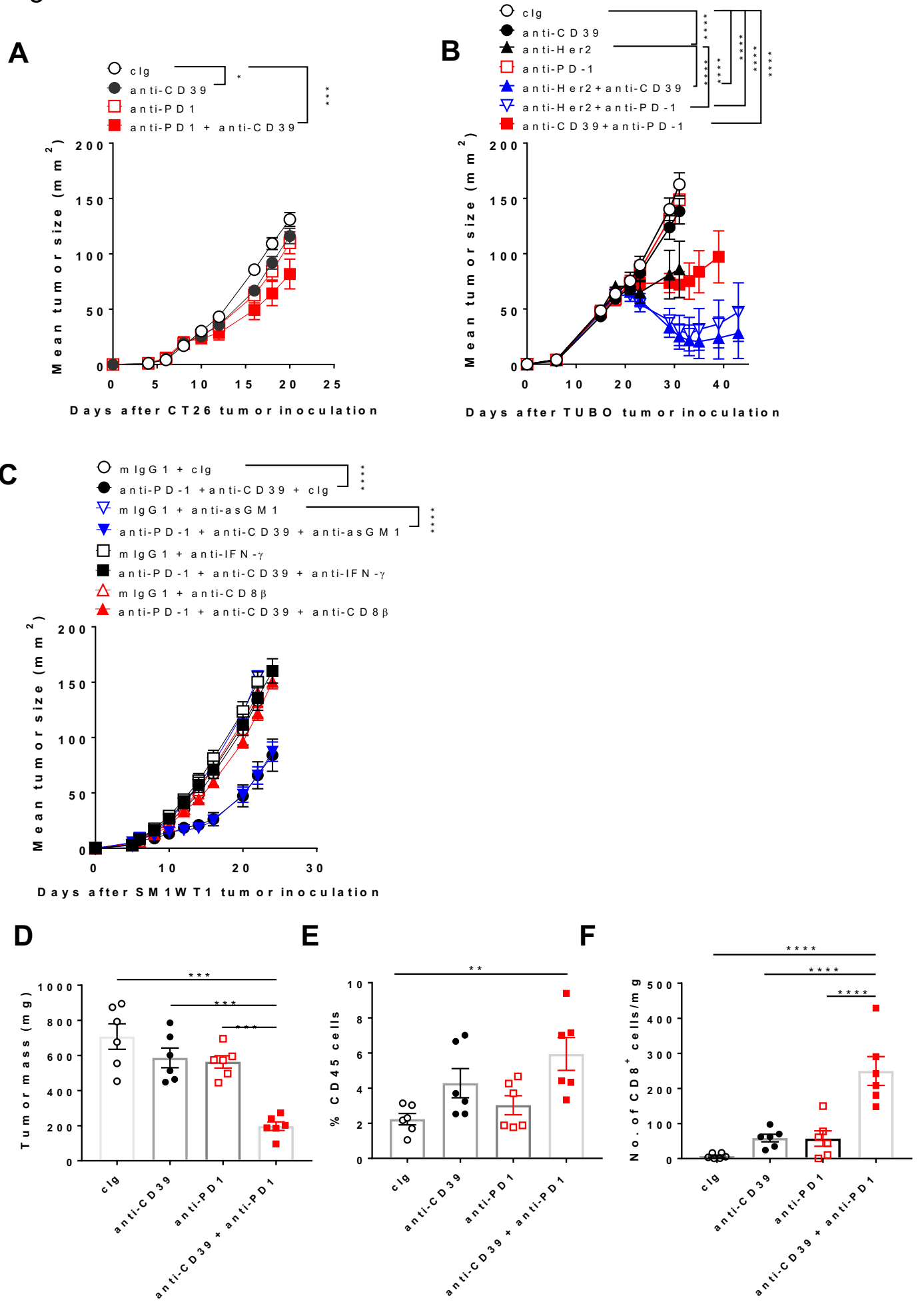
Figure S14. CD39 blockade sensitizes anti-PD1-resistant subcutaneous tumors. (A) Anti-CD39 sensitizes anti-PD1-resistant CT26 colon adenocarcinomas. Groups (n = 10/group) of BALB/c WT mice were injected s.c. with (**A**) CT26 (1 x 10^5) on day 0 and treated i.p. with cIg (200 μg), anti-CD39 (200 μg), anti-PD1 (250 μg) and combination of anti-CD39 and anti-PD1 (200 μg; 250 μg) as indicated on days 8, 11, 14, 17. **(B)** Anti-CD39 sensitizes anti-PD1-resistant TUBO mammary carcinomas. Groups (n = 7-8/group) of BALB/c WT mice were injected s.c. with TUBO (5 x 10^5) on day 0 and treated i.p with cIg (200 μg), anti-CD39 (200 μg), anti-PD1 (250 μg), anti-Her2 (7.16.4, 100 μg) alone and in various combinations as indicated on days 18,21,23, and 29. **(C)** Anti-CD39- and anti-PD1-mediated control of SM1WT1 is IFN-γ and CD8$^+$ T cell-dependent. Groups (n = 5/group) of WT mice were injected s.c. with SM1WT1 (1 x 10^6) on day 0 and treated i.p. with cIg (200 μg), anti-CD39 (200 μg), anti-PD1 (250 μg) on days 6, 9, 12, and 15 and some groups of mice were also treated i.p. with either cIg (100 μg), anti-asGM1 (50 μg,) anti-CD8β (100 μg) or anti-mIFN-γ (250 μg) on days 5, 6 13, and 20. Tumor sizes (mm^2) were measured at the indicated time points and presented as mean ± SEM. All experiments were performed once. Significant differences between the indicated groups were determined by a two-way ANOVA, followed by Tukey's multiple comparison test (* $P < 0.05$, *** $P < 0.001$, **** $P < 0.0001$). **(D-F)** From same experiment as Figure 5F, G. The tumors were collected on day 14, 48 h after the third dose. Graphs showing tumor weight **(D)**, summary bar graph of percentage of CD45$^+$ cells **(E)**, and numbers of CD8$^+$ T cell count per mg tumor mass **(F)**. Significant differences in percentage between the selected cell populations were determined by one-way ANOVA, followed by Tukey's multiple comparison test (** $P < 0.01$, *** $P < 0.001$, **** $P < 0.0001$).

Figure S15

A

HC.PmelKO
.TYRP1-
SFhg100

Cyclo

Pmel-1
T cells

CpG/pI:C

0   12   13   15 18 21 24   days

clg or anti-CD39

B

Percent survival

clg
anti-CD39

*
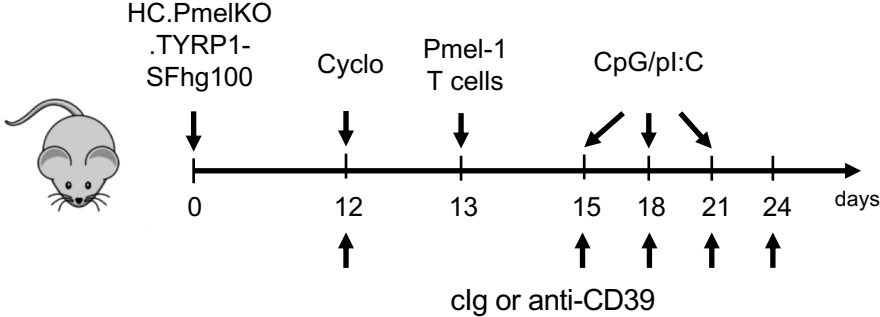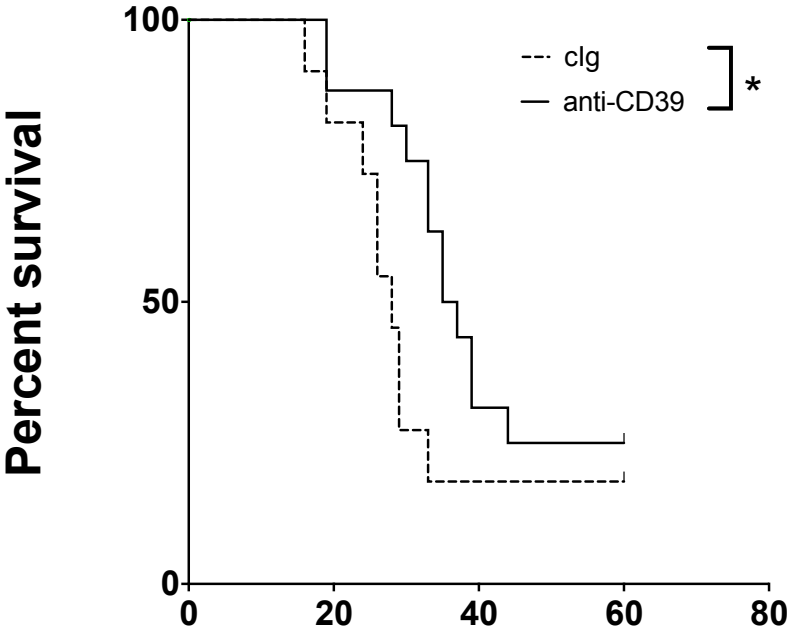
Days after HC.pMEL tumor inoculation

Figure S15. Anti-CD39 enhances the efficacy of adoptive cellular therapy against immune cell poor melanoma. (A) Experimental setup: WT mice were injected with HCmel12 melanoma expressing the human gp100 epitope under the control of the melanocytic lineage gene *Typr1* [HC.pMELKO.TYRP1-SFhg100, HC.pMEL)]. Once tumors were palpable, mice received a single dose of cyclophosphamide (Cyclo)(2 mg) followed by adoptive transfer of 10^6 pMEL-1 T cells and three intratumor injections of CpG/polyI:C (50 μg each). Cohorts of mice were randomly assigned to either receive control IgG (cIg) or anti-CD39 (B66) antibody. **(B)** Corresponding Kaplan-Meier-Plot showing overall survival of mice treated with ACT+cIg or ACT+anti-CD39 (n = 11 for cIg; n = 16 for anti-CD39). Significant differences between the indicated groups were determined Gehan-Breslow-Wilcoxon test (* $P < 0.05$).

A

BCL1 cells

B
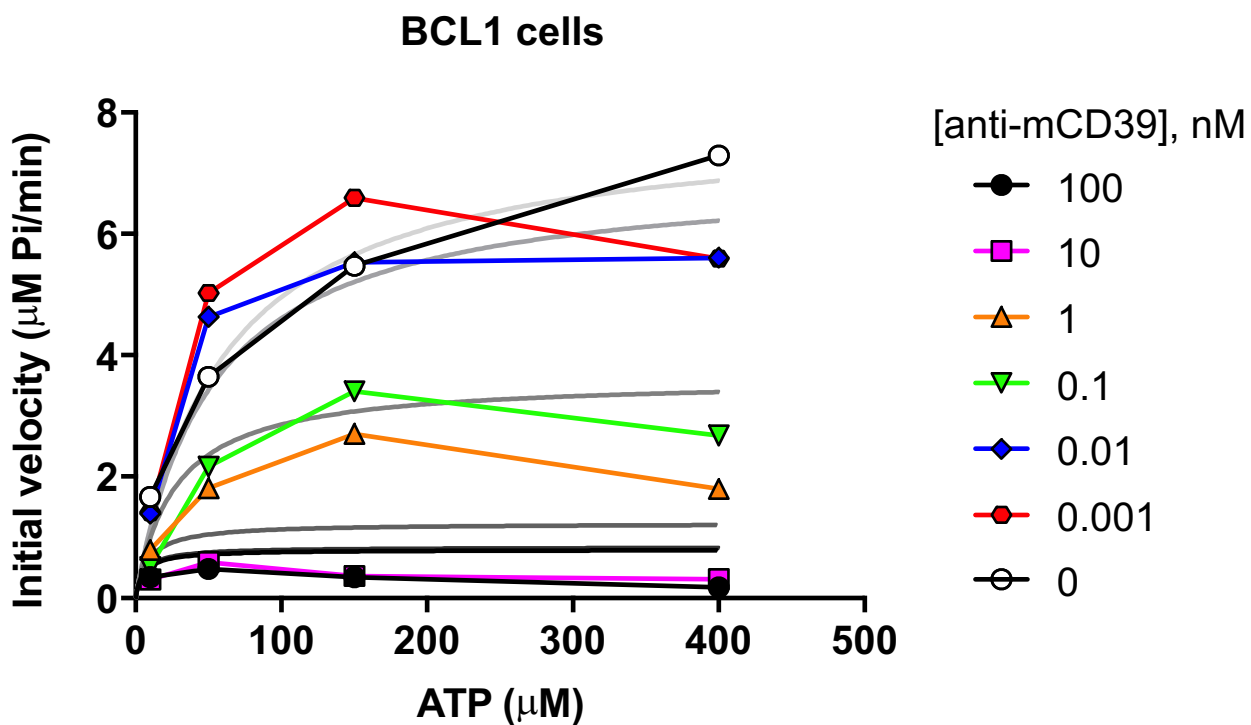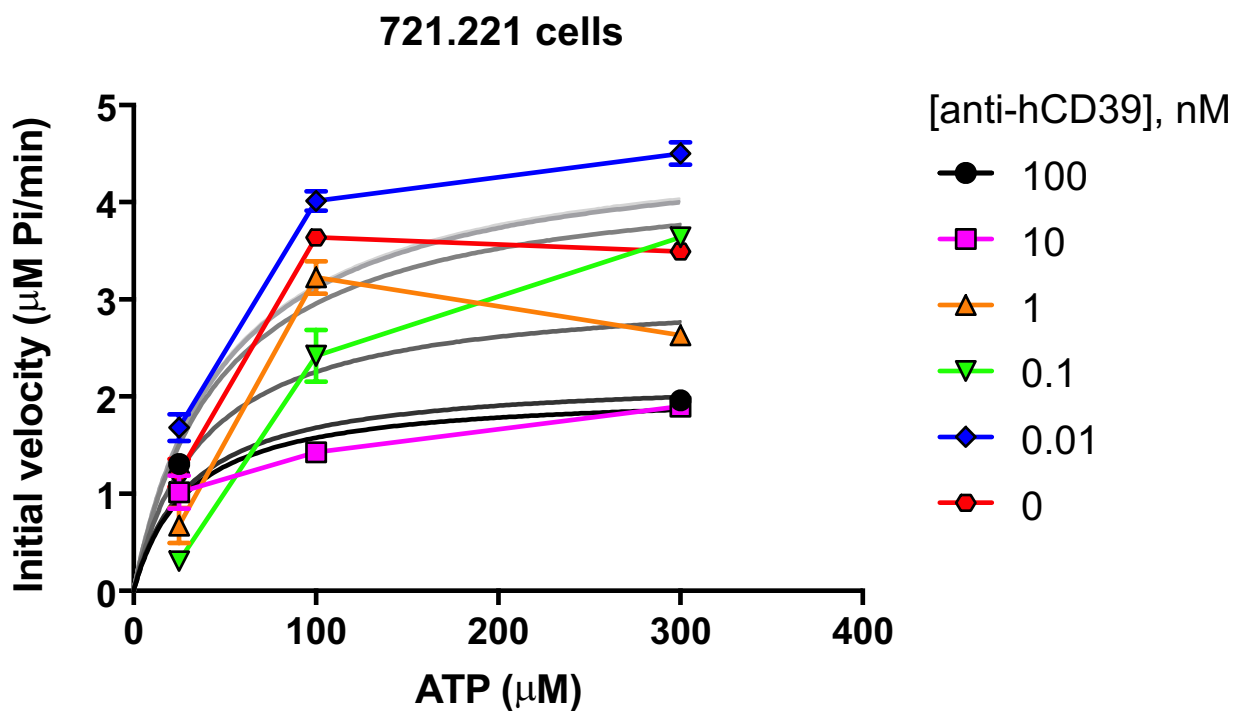
721.221 cells

Figure S16. Anti-mCD39 B66 and Anti-hCD39 TTX-030 allosterically inhibit CD39 ATPase activity. (**A**) Mouse cells endogenously expressing CD39 (BCL1 clone 5B1b) or (**B**) human cells endogenously expressing CD39 (721.221) were treated with anti-CD39 antibody and ATP and subsequent phosphate production monitored kinetically using the EnzChek Phosphate Assay Kit (Invitrogen, CAT# E-6646). Michaelis-Menten kinetic modeling was used to determine various kinetic parameters including V_{max} and K_{app}. These were in turn used in a set of mixed model inhibition equations to determine mechanism of inhibition of B66 and TTX-030. In both cases, it was determined that the mAbs inhibit CD39 ATP hydrolysis with an allosteric mechanism ($\alpha < 1$).

Figure S17
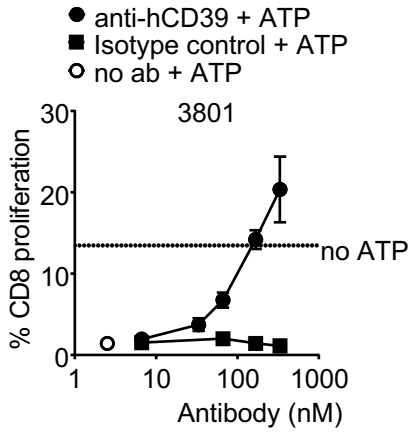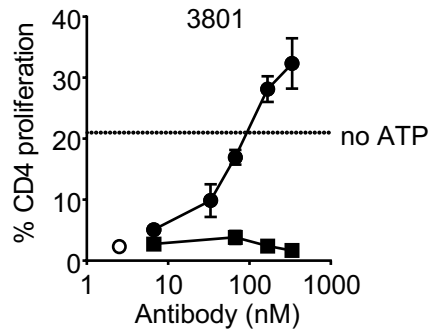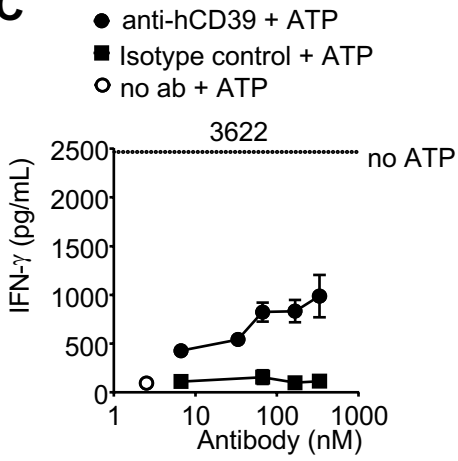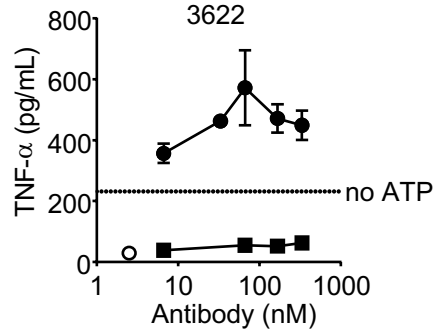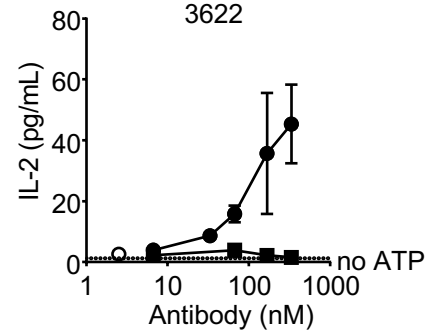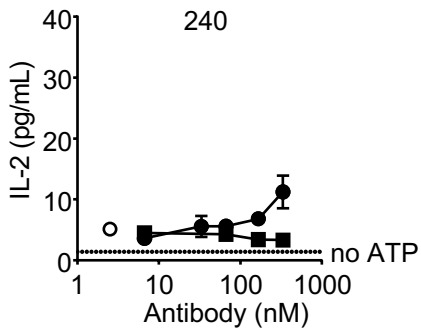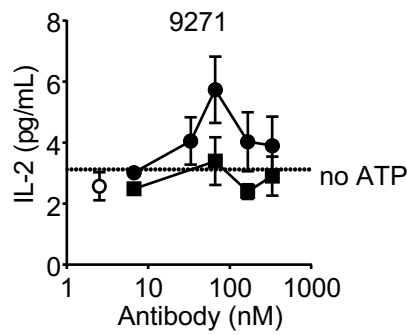
Figure S17. Anti-human CD39 enhances T cell proliferation and Th1 cytokine production. PBMCs from four different donors were harvested, stimulated with anti-CD3/anti-CD28, and assessed in triplicate for T cell proliferation and cytokine release in the presence and absence of ATP by flow cytometry. The graphs represent anti-hCD39-induced increased CD8 (**A**) and CD4 (**B**) T cell proliferation in the presence of ATP (donor 3801), and increased IFN-γ (**C**), TNF-α (**D**) and IL-2 **(E-G)** production in PBMCs (donors 3622, 240 and 9271), treated with anti-hCD39 in the presence of ATP.

Figure S18

A

LCL 043

LCL 039

isotype control

CD39-PE

CD39

CD39

B

SK-MEL-28

Isotype control

CD39-PE

CD39

C

○ cIg
● anti- hCD39

Mean tumor size (mm^2)

Days after SK-MEL-28 tumor inoculation
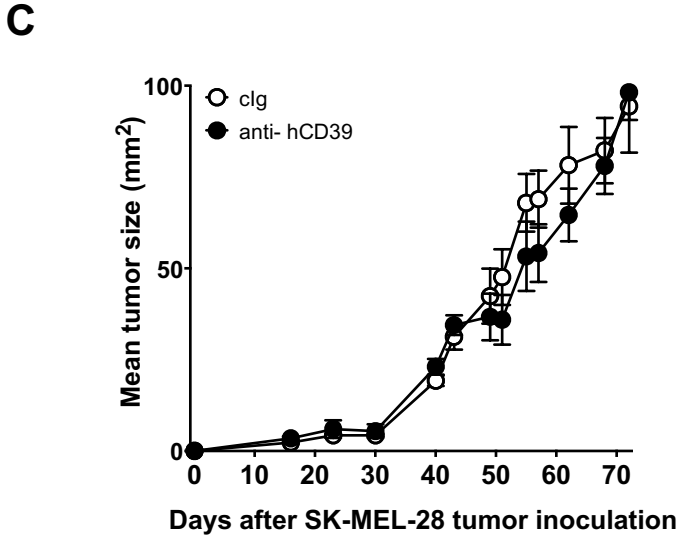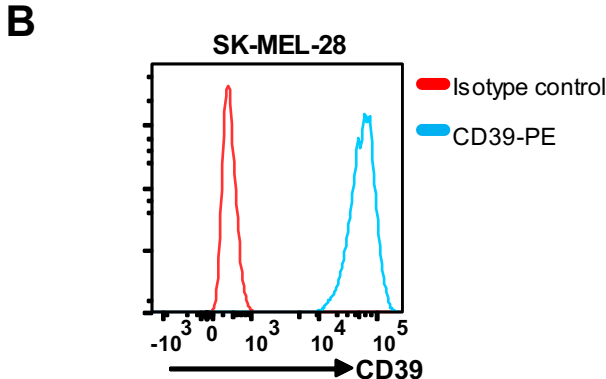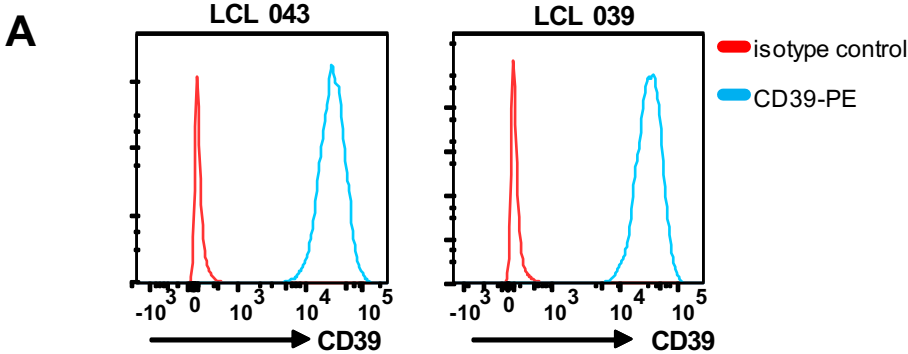
Figure S18. Human CD39. (A-B) Flow cytometry histograms showing CD39 expression on (**A**) lymphoblastoid cells LCL043, LCL039 or (**B**) SK-MEL-28 melanoma cells. (**C**) Groups (n = 7-8/group) of NRG mice were injected s.c. with SK-MEL-28 melanoma cells (2.5 x 10^6) and treated i.p. with cIg (250 µg) or anti-CD39 (250 µg) on days 44, 47, 49, 51, 54 and 56. Tumor sizes (mm^2) were measured at the indicated time points and presented as mean ± SEM. Representative data from two independent experiments.

Figure S19
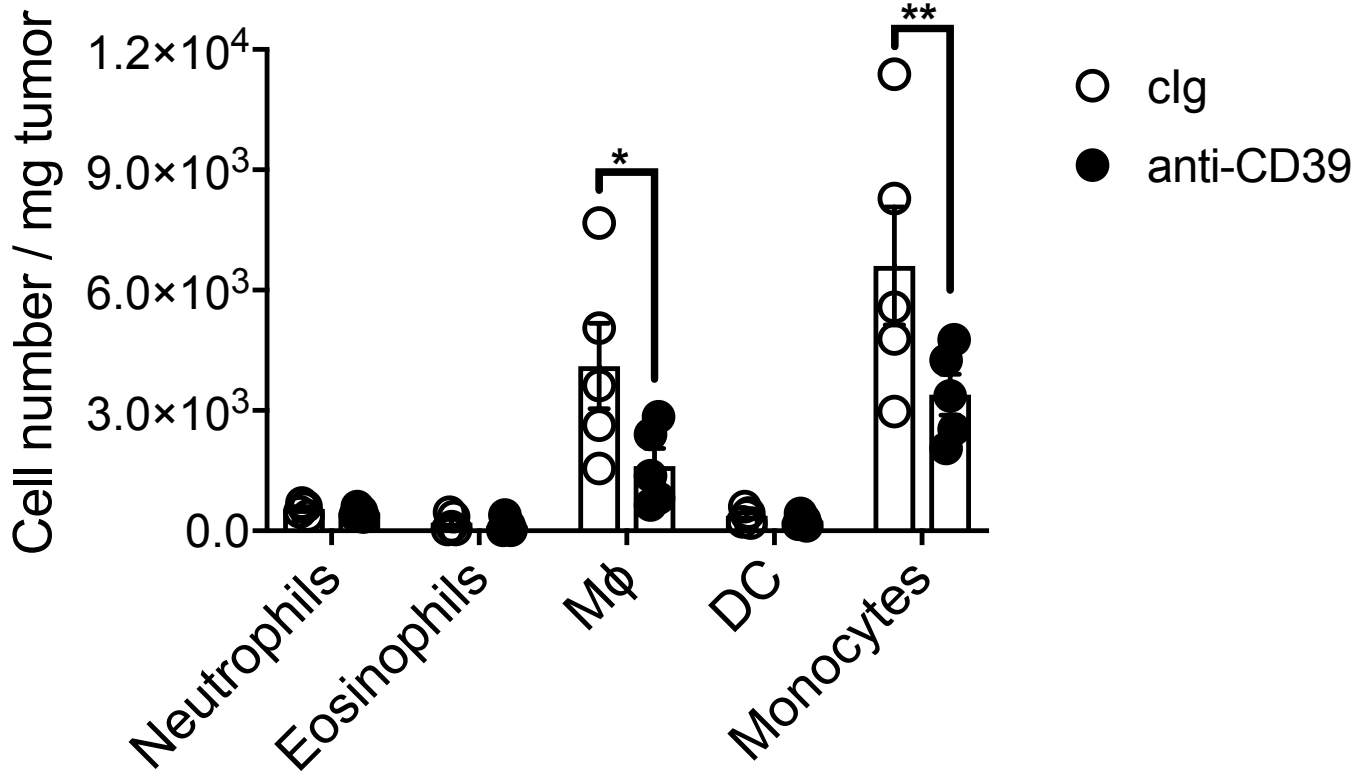
Figure S19. Flow cytometry shows macrophage reduction in RM-1 tumors after anti-CD39 treatment. Groups (n = 5/group) of WT mice were injected s.c. with RM-1 prostate carcinoma cells (5 x 10^4) on day 0 and treated i.p with cIg (200 μg) or anti-CD39 (200 μg) on days 6. Tumor samples were collected on day 8 and processed for single cell suspensions then subjected to flow cytometry. Summary bar graphs of numbers of myeloid populations in tumor, as mean ± SEM with individual values shown. (* P < 0.05, ** P < 0.01, determined by a two-way ANOVA, followed by Sidak's multiple comparison test). Data represents one experiment.

Table S1 Top 150 differentially regulated genes in MC38 tumors treated with cIg or anti-CD39 antibody as shown in Figure 3C.

Gene.Name	Associated.Gene.Name	logFC	PValue	Padj
ENSMUSG00000007877	Tcap	1.84315765	4.52E-15	1.08E-12
ENSMUSG00000018893	Mb	1.78940325	2.79E-12	3.18E-10
ENSMUSG00000069622	Gm10273	0.57156842	2.88E-12	3.26E-10
ENSMUSG00000024371	C2	1.61698752	5.00E-19	2.95E-16
ENSMUSG00000001056	Nhp2	0.50561928	4.24E-11	3.47E-09
ENSMUSG00000006360	Crip1	0.63564797	5.96E-14	1.08E-11
ENSMUSG00000057322	Rpl38	0.53745189	4.11E-11	3.41E-09
ENSMUSG00000025283	Sat1	0.45430193	6.95E-11	5.48E-09
ENSMUSG00000037646	Vps13b	-0.6455412	1.55E-17	6.68E-15
ENSMUSG00000022812	Gsk3b	-0.5464004	3.56E-14	7.12E-12
ENSMUSG00000036273	Lrrk2	-0.5978489	1.69E-12	2.06E-10
ENSMUSG00000036792	Mbd5	-0.6413971	1.20E-13	1.91E-11
ENSMUSG00000047414	Flrt2	-0.518313	5.32E-13	7.95E-11
ENSMUSG00000019726	Lyst	-1.048263	8.89E-24	1.11E-20
ENSMUSG00000035284	Vps13c	-0.8443381	9.15E-13	1.23E-10
ENSMUSG00000022641	Bbx	-0.6020853	7.63E-14	1.31E-11
ENSMUSG00000041702	Btbd7	-0.922413	6.32E-17	2.28E-14
ENSMUSG00000067336	Bmpr2	-1.5092389	2.80E-29	1.57E-25
ENSMUSG00000031529	Tnks	-1.0950279	3.75E-25	7.01E-22
ENSMUSG00000034342	Cbl	-1.4523348	3.94E-27	1.10E-23
ENSMUSG00000028246	6230409E13Rik	-0.7027988	2.59E-12	2.99E-10
ENSMUSG00000052812	Atad2b	-1.0771254	2.02E-17	8.37E-15
ENSMUSG00000033855	Ston1	-0.7578346	5.67E-13	8.35E-11
ENSMUSG00000036109	Mbnl3	-1.0663549	1.03E-13	1.71E-11
ENSMUSG00000033960	9430020K01Rik	-0.6637831	8.40E-13	1.15E-10
ENSMUSG00000038024	Dennd4c	-0.5895309	3.71E-12	3.99E-10
ENSMUSG00000094410	Zbed6	-1.4501981	1.44E-25	3.23E-22
ENSMUSG00000005886	Ncoa2	-0.6074981	6.76E-13	9.70E-11
ENSMUSG00000025949	Pikfyve	-0.8992978	8.83E-15	2.02E-12
ENSMUSG00000047036	Zfp445	-0.8754088	1.54E-12	1.92E-10
ENSMUSG00000096401	AC241392.2	-0.8434265	3.65E-12	3.99E-10
ENSMUSG00000069892	9930111J21Rik2	-0.845818	7.74E-19	4.33E-16
ENSMUSG00000022306	Zfpm2	-0.5482655	1.25E-10	9.34E-09
ENSMUSG00000033799	BC016423	-0.5544077	7.25E-11	5.63E-09
ENSMUSG00000030180	Kdm5a	-0.5260105	1.00E-11	9.77E-10

ENSMUSG00000037416	Dmxl1	-0.7724239	4.04E-15	9.85E-13
ENSMUSG00000020181	Nav3	-0.9337723	1.60E-19	1.20E-16
ENSMUSG00000038151	Prdm1	-0.7348829	3.82E-12	4.08E-10
ENSMUSG00000000628	Hk2	-0.488244	6.16E-11	4.93E-09
ENSMUSG00000025612	Bach1	-0.5262225	1.94E-11	1.78E-09
ENSMUSG00000033792	Atp7a	-1.1270831	4.98E-19	2.95E-16
ENSMUSG00000030660	Pik3c2a	-0.5942181	2.36E-14	4.99E-12
ENSMUSG00000040021	Lats1	-0.5127307	1.19E-10	8.99E-09
ENSMUSG00000039087	Rreb1	-0.7009343	4.17E-14	8.06E-12
ENSMUSG00000049470	Aff4	-0.6468274	7.08E-14	1.25E-11
ENSMUSG00000042473	Tbc1d8b	-0.7144496	3.18E-11	2.83E-09
ENSMUSG00000039286	Fndc3b	-0.5161241	3.20E-12	3.58E-10
ENSMUSG00000022883	Robo1	-0.6808323	2.58E-13	4.01E-11
ENSMUSG00000054387	Mdm4	-0.8795125	1.57E-12	1.94E-10
ENSMUSG00000046230	Vps13a	-0.7583028	1.53E-14	3.36E-12
ENSMUSG00000025326	Ube3a	-0.5874177	4.46E-12	4.64E-10
ENSMUSG00000021756	Il6st	-0.5558173	2.20E-12	2.59E-10
ENSMUSG00000055320	Tead1	-1.301947	2.15E-30	2.41E-26
ENSMUSG00000034636	Zyg11b	-0.4959564	1.17E-10	8.93E-09
ENSMUSG00000053877	Srcap	-1.3204004	2.04E-15	5.43E-13
ENSMUSG00000034218	Atm	-0.8619404	9.30E-18	4.16E-15
ENSMUSG00000047497	Adamts12	-1.0162726	1.41E-11	1.35E-09
ENSMUSG00000048279	Sacs	-0.7255095	4.22E-11	3.47E-09
ENSMUSG00000024542	Cep192	-0.6130059	3.34E-13	5.05E-11
ENSMUSG00000069793	Slfn9	-0.6637468	2.57E-12	2.99E-10
ENSMUSG00000026872	Zeb2	-0.6466166	1.55E-11	1.45E-09
ENSMUSG00000038371	Sbf2	-0.5533413	4.91E-12	4.96E-10
ENSMUSG00000039477	Tnrc18	-0.8138057	1.23E-15	3.36E-13
ENSMUSG00000026313	Hdac4	-0.9203918	3.83E-11	3.25E-09
ENSMUSG00000046138	9930021J03Rik	-0.7133291	1.54E-12	1.92E-10
ENSMUSG00000061436	Hipk2	-0.9124621	2.65E-18	1.41E-15
ENSMUSG00000034610	Zcchc11	-0.502338	6.91E-13	9.80E-11
ENSMUSG00000033396	Spg11	-0.4988122	1.96E-11	1.78E-09
ENSMUSG00000058690	Gcap14	-0.5432047	1.13E-12	1.51E-10
ENSMUSG00000057335	Cep170	-0.6342088	1.60E-16	5.14E-14
ENSMUSG00000037876	Jmjd1c	-0.6932789	5.98E-14	1.08E-11
ENSMUSG00000031540	Myst3	-0.7159131	3.12E-17	1.25E-14
ENSMUSG00000022141	Nipbl	-0.7041469	3.05E-16	9.00E-14
ENSMUSG00000039967	Zfp292	-0.7056634	4.32E-14	8.20E-12

ENSMUSG00000003119	Cdk12	-0.652897	2.18E-13	3.44E-11
ENSMUSG00000041852	Tcf20	-0.5490693	1.72E-12	2.08E-10
ENSMUSG00000034751	Mast4	-0.675687	4.75E-12	4.83E-10
ENSMUSG00000051149	Adnp	-1.2889419	6.18E-17	2.28E-14
ENSMUSG00000036202	Rif1	-0.6079938	7.95E-11	6.14E-09
ENSMUSG00000032740	Ccdc88a	-0.6263009	3.83E-11	3.25E-09
ENSMUSG00000022521	Crebbp	-0.8241118	5.66E-14	1.06E-11
ENSMUSG00000061755	Bod1l	-0.632616	1.20E-10	8.99E-09
ENSMUSG00000040225	Prrc2c	-1.0339487	7.83E-18	3.65E-15
ENSMUSG00000019907	Ppp1r12a	-0.6298676	4.47E-12	4.64E-10
ENSMUSG00000036550	Cnot1	-0.4963522	4.04E-11	3.40E-09
ENSMUSG00000019820	Utrn	-0.6246233	8.55E-12	8.39E-10
ENSMUSG00000005871	Apc	-0.5909858	1.11E-10	8.49E-09
ENSMUSG00000037270	4932438A13Rik	-0.7040642	3.32E-15	8.26E-13
ENSMUSG00000034377	Tulp4	-0.5465416	8.12E-12	8.05E-10
ENSMUSG00000031441	Atp11a	-0.528958	5.88E-11	4.74E-09
ENSMUSG00000037112	Sik2	-0.6191487	1.23E-11	1.19E-09
ENSMUSG00000022263	Trio	-0.6239415	3.81E-11	3.25E-09
ENSMUSG00000040524	Zfp609	-0.6794061	7.88E-15	1.84E-12
ENSMUSG00000020640	Itsn2	-0.6132294	6.65E-12	6.65E-10
ENSMUSG00000043940	Wdfy3	-0.6824764	1.04E-13	1.71E-11
ENSMUSG00000037487	Ubr5	-0.5264442	3.73E-11	3.24E-09
ENSMUSG00000015501	Hivep2	-0.585124	6.59E-13	9.59E-11
ENSMUSG00000057230	Aak1	-1.2529859	9.91E-16	2.77E-13
ENSMUSG00000028487	Bnc2	-0.940397	1.11E-14	2.50E-12
ENSMUSG00000038679	Trps1	-0.6059365	1.12E-13	1.82E-11
ENSMUSG00000021782	Dlg5	-0.5703048	3.30E-11	2.88E-09
ENSMUSG00000021767	Myst4	-0.70999	6.88E-11	5.47E-09
ENSMUSG00000068284	Gm608	-0.7013207	2.61E-11	2.34E-09
ENSMUSG00000019841	Rev3l	-0.6890561	1.46E-11	1.39E-09
ENSMUSG00000028053	Ash1l	-0.7291701	3.75E-14	7.36E-12
ENSMUSG00000074305	C230081A13Rik	-0.6721642	1.90E-14	4.08E-12
ENSMUSG00000070565	Rasal2	-0.7054422	7.51E-13	1.05E-10
ENSMUSG00000041444	Arhgap32	-0.7818615	4.25E-12	4.49E-10
ENSMUSG00000030516	Tjp1	-0.6360077	3.71E-12	3.99E-10
ENSMUSG00000034297	Med13	-0.6432913	7.13E-14	1.25E-11
ENSMUSG00000029313	Aff1	-0.6592621	3.36E-14	6.84E-12
ENSMUSG00000022016	Akap11	-0.5441697	3.28E-11	2.88E-09
ENSMUSG00000018076	Med13l	-0.7493125	7.39E-17	2.59E-14

ENSMUSG00000027799	Nbea	-0.7459495	9.51E-17	3.23E-14
ENSMUSG00000036698	Eif2c2	-1.0030473	6.08E-25	9.73E-22
ENSMUSG00000021831	Ero1l	-0.8357147	1.40E-16	4.61E-14
ENSMUSG00000027820	Mme	-0.779831	5.16E-11	4.19E-09
ENSMUSG00000036155	Mgat5	-1.0285818	2.89E-16	8.76E-14
ENSMUSG00000054008	Ndst1	-0.6382115	3.56E-12	3.95E-10
ENSMUSG00000028030	Tbck	-0.8834419	1.55E-11	1.45E-09
ENSMUSG00000039952	Dag1	-0.7110282	3.00E-15	7.64E-13
ENSMUSG00000060012	Kif13b	-0.9032526	1.47E-12	1.87E-10
ENSMUSG00000042390	Gatad2b	-1.0849678	4.64E-22	5.20E-19
ENSMUSG00000053007	Creb5	-1.053161	1.93E-12	2.30E-10
ENSMUSG00000032487	Ptgs2	-0.7902567	2.10E-11	1.90E-09
ENSMUSG00000041324	Inhba	-1.1335198	6.83E-21	5.89E-18
ENSMUSG00000079575	Rbpsuh-rs3	-1.151103	1.34E-24	1.87E-21
ENSMUSG00000019947	Arid5b	-1.0683836	2.65E-16	8.25E-14
ENSMUSG00000073016	Uprt	-0.9924767	1.15E-12	1.51E-10
ENSMUSG00000025017	Pik3ap1	-0.619213	1.73E-11	1.60E-09
ENSMUSG00000069607	Cd300lh	-0.7785191	7.16E-11	5.61E-09
ENSMUSG00000079685	Ulbp1	-0.9958741	3.14E-13	4.82E-11
ENSMUSG00000052414	Atf7	-1.219725	1.31E-12	1.68E-10
ENSMUSG00000063550	Nup98	-0.7725928	3.54E-17	1.37E-14
ENSMUSG00000040274	Cdk6	-0.9396621	3.46E-16	9.95E-14
ENSMUSG00000069893	9930111J21Rik1	-1.4933908	2.31E-28	8.64E-25
ENSMUSG00000029202	Pds5a	-0.8007329	2.78E-18	1.41E-15
ENSMUSG00000037533	Rapgef6	-0.6396602	4.68E-12	4.81E-10
ENSMUSG00000023845	Lnpep	-1.1175084	7.86E-20	6.29E-17
ENSMUSG00000039704	Lmbrd2	-1.3802661	8.79E-22	8.21E-19
ENSMUSG00000021952	Xpo4	-1.0035331	2.20E-15	5.73E-13
ENSMUSG00000035133	Arhgap5	-0.9957967	5.14E-22	5.23E-19
ENSMUSG00000035898	Uba6	-0.7107274	9.47E-14	1.61E-11
ENSMUSG00000024298	Zfp871	-1.524904	7.75E-13	1.07E-10
ENSMUSG00000075470	Alg10b	-0.9623805	4.72E-18	2.30E-15
ENSMUSG00000070639	Lrrc8b	-1.1570397	2.43E-19	1.70E-16
ENSMUSG00000021466	Ptch1	-1.1699887	2.91E-14	6.04E-12
ENSMUSG00000063895	Nupl1	-0.564427	4.10E-11	3.41E-09
ENSMUSG00000020961	Ston2	-0.9794443	1.20E-12	1.57E-10
ENSMUSG00000033624	Pdpr	-1.1331289	2.72E-19	1.79E-16

Table S2

Supplementary Table 2 - Summary of antibody specific IHC conditions				
SI No	Target	Ag Retrieval & pH	Primary Ab clone	Primary Ab dilution
1	CD8	Dako Target Retrieval Solution, pH 9	C8/144B	1:200
2	CD39	Dako Target Retrieval Solution, pH 9	OTI2B10	1:200
3	PD1	Dako Target Retrieval Solution, pH 6	NAT105	1:100
4	CD19	Dako Target Retrieval Solution, pH 9	EPR5906	1:200